Titre: Title:	Etudes expérimentales du remplissage d'un moule pour le procédé CRTM et de la compressibilité de coeur en mousse pour les procédés RTM et SRIM
Auteur: Author:	Stéphane Wirth
Date:	1997
Type:	Mémoire ou thèse / Dissertation or Thesis
Référence: Citation:	Wirth, S. (1997). Etudes expérimentales du remplissage d'un moule pour le procédé CRTM et de la compressibilité de coeur en mousse pour les procédés RTM et SRIM [Mémoire de maîtrise, École Polytechnique de Montréal]. PolyPublie. https://publications.polymtl.ca/6851/

UNIVERSITÉ DE MONTRÉAL

ÉTUDES EXPÉRIMENTALES DU REMPLISSAGE D'UN MOULE POUR LE PROCÉDÉ CRTM ET DE LA COMPRESSIBILITÉ DE COEUR EN MOUSSE POUR LES PROCÉDÉS RTM ET SRIM

STÉPHANE WIRTH

DÉPARTEMENT GÉNIE MÉCANIQUE

ÉCOLE POLYTECHNIQUE DE MONTRÉAL

MÉMOIRE PRÉSENTÉ EN VUE DE L'OBTENTION

DU DIPLÔME DE MAÎTRISE ÈS SCIENCES APPLIQUÉES

(GÉNIE MÉCANIQUE)

DÉCEMBRE 1997

National Library
of Canada

Acquisitions and
Bibliographic Services

395 Wellington Street
Ottawa ON K1A 0N4
Canada

Bibliothèque nationale
du Canada

Acquisitions et
services bibliographiques

395, rue Wellington
Ottawa ON K1A 0N4
Canada

Your file Votre référence

Our file Notre référence

0-612-37468-8

Canada

UNIVERSITÉ DE MONTRÉAL

ÉCOLE POLYTECHNIQUE DE MONTRÉAL

Ce mémoire intitulé :

ÉTUDES EXPÉRIMENTALES DU REMPLISSAGE D'UN MOULE POUR LE PROCÉDÉ CRTM ET DE LA COMPRESSIBILITÉ DE COEUR EN MOUSSE POUR LES PROCÉDÉS RTM ET SRIM

présenté par : WIRTH Stéphane

en vue de l'obtention du diplôme de : Maîtrise ès sciences appliquées

a été dûment accepté par le jury d'examen constitué de :

M. TROCHU François, Ph.D., président

M. GAUVIN Raymond, Ph.D., membre et directeur de recherche

M. SANCHAGRIN Bernard, Ph.D., membre

Pour mes parents...

REMERCIEMENTS

Cet ouvrage a été réalisé au Centre de Recherche Appliqué sur les polymères (CRASP) de l'École Polytechnique de Montréal.

L'auteur voudrait remercier le FCAR (Fonds pour la formation de chercheurs et l'aide à la recherche du Canada) pour le support financier donné à M. Stéphane Wirth, le Centre National de Recherche du Canada (CNRC) pour son aide financière, le SRL (Scientific Research Laboratory) de la compagnie Ford Motor pour son assistance et pour l'utilisation de son équipement de moulage et la compagnie APX pour l'utilisation de leurs installations de fabrication de coeur de mousse. Également, l'auteur voudrait remercier particulièrement la collaboration des personnes suivantes pour leurs conseils judicieux fournis lors des essais expérimentaux et la rédaction de cet ouvrage: Dr. Raymond Gauvin (École Polytechnique de Montréal), Dr. François Trochu (École Polytechnique de Montréal) et Dr. Ken Kendall (Ford Motor Company).

L'auteur tient également à remercier le département de génie mécanique, plus particulièrement les techniciens de la section design et machines sous la direction de Monsieur François Morin. Les essais expérimentaux effectués dans les laboratoires de l'École Polytechnique n'auraient pu se concrétiser sans la collaboration de Messieurs Jacques Beausoleil et Richard Dallaire. Sans oublier

Lyne Loiselle pour son aide apportée tout au long du cheminement de ma maîtrise.

RÉSUMÉ

Deux des procédés les plus utilisés pour le moulage de pièces composites avec des renforts de fibre de verre sont les procédés RTM (Resin Transfer Molding) et SRIM (Structural Reaction Injection Molding). Ces systèmes d'injection sont maintenant couramment utilisés dans le domaine des transports automobiles et récréatifs. Dans un premier temps, le procédé consiste à placer un renfort dans un moule. Par la suite, celui-ci est fermé et l'on injecte une résine à basse viscosité afin de bien mouiller les fibres. Une résine vinyl-ester ou polyester est utilisée pour le RTM et une résine polyuréthanne est employée pour le procédé SRIM.

La première partie de cet ouvrage consiste en l'étude expérimentale du moulage de pièces composites avec un coeur de mousse. Les phénomènes étudiés sont la déformation des noyaux de mousse et la compaction des renforts lors d'une injection RTM et SRIM. Le moulage à haut débit SRIM a pour effet de bâtir une importante pression dans le moule, de déplacer et de déformer les coeurs de mousse et de varier la perméabilité locale du renfort lorsque celui-ci est compacté sur les parois du moule. Par conséquent, la loi de Darcy linéaire ne s'applique pas dans ces cas précis, car la perméabilité « K » varie en fonction du temps. Également, des zones sèches dans les renforts peuvent êtres observées dans la pièce finale. L'étude de ces phénomènes a été effectuée à l'aide de

deux moules en acier équipés de capteurs de pression. Des coeurs de mousse polyuréthanne de différentes densités ont été utilisés avec deux types de renfort : un mat de fibres de verre aléatoires continus et un tissage de fibres de verre ±45°/ 0°. Le moulage RTM n'a pas donné de résultats intéressants en ce qui concerne la déformation des coeurs de mousse. L'injection SRIM a causé une déformation évidente des noyaux de mousse de basses densités ainsi qu'une compaction des renforts. Des simulations pour les essais expérimentaux ont été effectués sur le logiciel RTMFLOT de l'École Polytechnique de Montréal afin de prédire la montée de pression au niveau de la tête d'injection.

La seconde partie de l'ouvrage traite du procédé CRTM (Compression Resin Transfer Molding) et de ses variantes possibles. Tout comme le procédé RTM, une préforme de fibre de verre est placée dans un moule dans lequel on injecte une résine. La différence réside dans le fait que le moule est partiellement ouvert durant l'injection. Par la suite, le moule est fermé afin de bien mouiller les renforts. L'avantage de cette nouvelle technique est de pouvoir atteindre une plus grande concentration de fibre pour une même épaisseur comparativement au RTM. La première série d'expérimentations utilisait une préforme de fibre de verre thermoformée placée dans un moule légèrement ouvert. Tout de suite après l'injection de la résine, le moule était fermé. Le temps d'injection était très court. La seconde série d'expérimentations utilisait des mats de fibres de verre aléatoires continus afin de remplir la cavité entrouverte du moule.

Contrairement à la première série d'expérimentations, la résine était injectée en même temps que le moule était fermé. Le résultats obtenus pourront être utilisés afin de simuler une déformation d'un coeur de mousse et une compaction des renforts.

ABSTRACT

Two of the most used Liquid Composite Molding (LCM) processes to produce economic high performance composites are Resin Transfer Molding (RTM) and Structural Reaction Injection Molding SRIM. These systems are known commonly used in the aerospace, automotive and recreative transportation industries. In these processes, reinforcement is placed in a closed mold cavity. Then, a liquid resin is injected to wet the fabric. This work wills basically treats of these two injection systems using some modifications.

The first part of the work deals with the core crushing and core movement in RTM and SRIM foam cored composite parts. When molding a foam cored composite part at high flow rates using an SRIM system, the following related effects can be observe: high molding pressures, core shifting, core crushing, variable permeability and reinforcement compaction. Because of the variable permeability in such conditions, the linear Darcy law does not apply for flow simulation. Finally, all this can easily result in dry spot defects. To study the various problems occurring in the molding of foam cored composite parts, two molds equipped with pressure transducers were used. For the experiments, continuous strand mat and braided glass fabrics with ±45° and axial (0°) filaments was used with Polyurethane foam of variable density. RTM process gave no significant core deformation. With the SRIM system, results showed a

non-negligible core deformation at some foam densities. The results revealed the dominance of the core shifting and fabric compaction over core crushing. The flow simulation software RTMFLOT developed in our laboratory and based on a linear Darcy Law was used with these complex cases. The simulation results gave a good approximation of the gate pressure during filling.

The second part of the work deal basically with the Compression Resin Transfer Molding (CRTM). In that process, like in RTM, the fiber preform is preplaced in a mold and then, a liquid resin is injected. In CRTM however, the mold is kept slightly open during the resin injection. Once the necessary amount of resin is injected, the final closing is done and the resin filled the entire cavity. The main advantage of this technique is to reduce the necessary injection pressure and to ease the molding of parts with high fiber. Two types of experiments were performed. The first series use a thermoformed glass fiber preform placed in a slightly open cavity. The resin was then injected in this open cavity. The mold was then closed to final part thickness. In this case, the resin injection time was extremely short and most of filling and wetting time was elevated to the final closing of the cavity. The second set of experiments used continuous strand glass fiber mat to completely fill partially closed mold cavities. As oppose to the previous experiments, in this case, the cavity was closed during the resin injection. The closing time was chosen in such a way that filling and closing occur simultaneously. The data gathered with these experiments could also be

used to validate the modeling of foam core parts molding when resin pressure crushes cores.

TABLES DES MATIÈRES

LISTE DES TABLEAUX

LISTE DES FIGURES

LISTE DES SIGLES ET ABRÉVIATIONS

a :	Longueur (m)
A :	Surface (m^2)
A_s :	Constante d'élasticité
b :	Largeur (m)
C_f :	Épaisseur finale du coeur de mousse (mm)
C_i :	Épaisseur initiale du coeur de mousse (mm)
D_c :	Déformation du coeur de mousse (mm)
D_cx :	Déformation du coeur de mousse dans la direction X, largeur (mm)
D_cy :	Déformation du coeur de mousse dans la direction Y, hauteur (mm)
E :	Module de flexion (Pa)
E1 :	Module de compression premier (Pa)
E2 :	Module de compression second (Pa)
F :	Épaisseur de l'écoulement du dessus (mm)
h :	Épaisseur du renfort (mm)
k :	Pente de compressibilité du renfort (Pa/m)
K :	Perméabilité (m^2)
K_z :	Constante de Kozeny
L :	Épaisseur du laminé (mm)
L_{init} :	Épaisseur du laminé initiale (mm)
Lx_1 , Lx_2 :	Épaisseurs du laminé dans la direction X du coeur de mousse (mm)

Ly_1 , Ly_2 :	Épaisseurs du laminé dans la direction Y du coeur de mousse (mm)
M :	Masse (kg)
M_i :	Ouverture de la cavité du moule plaque (mm)
Mx :	Déplacement du coeur de mousse dans la direction X, largeur (mm)
My :	Déplacement du coeur de mousse dans la direction Y, largeur (mm)
n :	Exposant de la loi de puissance
P :	Pression du fluide (Pa)
P_{mn} :	Distribution de pression (Pa)
P1 - P17 :	Capteurs de pression
Q :	Débit volumétrique ($m^3 \bullet s^{-1}$)
R_z :	Rayon moyen des fibres (m)
Re_k :	Nombre de Reynolds selon la perméabilité
t :	Temps (s)
T :	Température (°C)
T1 :	Thermocouple
v :	Volume (m^3)
V :	Vitesse de l'écoulement (m/s)
V_f :	Taux de fibre (%)
V_m :	Taux de fibre moyen (%)
V_o :	Taux de fibre initial (%)
w :	Flèche (m)
β :	Rapport de la longueur sur la hauteur des fibres

ϕ :	Porosité du milieu
γ :	Coefficient de poisson
ρ :	Densité (kg/m^3)
μ :	Viscosité dynamique ($N \bullet s \bullet m^{-2}$)
$\delta p / \delta x$:	Gradient de pression ($N \bullet m^{-1}$)
$\Delta P_f / \Delta L$:	Gradient de pression ($N \bullet m^{-1}$)

LISTE DES ANNEXES

INTRODUCTION

Les matériaux composites sont de plus en plus répandus pour la fabrication de structures dans le domaine des transports tel que l'automobile et les véhicules récréatifs. Le procédé RTM (Resin Transfer Molding) permet de fabriquer des pièces géométriques complexes en fibre de verre avec un équipement peu coûteux. Le procédé RTM consiste a injecter une résine thermodurcissable, de type polyester ou vinyl-ester, à l'intérieur d'un moule contenant une préforme en fibre de verre. La réaction de polymérisation terminée, le moule est ouvert et la pièce est éjectée. La pression d'injection étant faible, soit environ 500 KPa, le RTM permet d'utiliser des moules légers et économiques. Le RTM permet de produire une vaste gamme de pièces structurales permettant d'utiliser des coeurs de mousse ainsi que d'orienter les fibres selon des directions préférentielles. L'utilisation d'un moule fermé réduit les émanations de styrènes nuisibles à la santé des travailleurs. Le RTM ne possède pas encore la technologie nécessaire pour produire un volume de pièce élevée (> 100000 pièces par an). Il est utilisé pour une production variant entre 100 et 10000 pièces. Son principal désavantage étant sa faible réactivité de sa résine et la difficulté de produire des pièces de grandes épaisseurs.

Le procédé SRIM est une variante du procédé RTM au niveau de la résine. Pour le SRIM, une résine de type polyuréthanne est injectée à haut débit

dans la cavité du moule contenant la préforme. L'avantage du SRIM est que la résine polyuréthanne possède une réactivité chimique beaucoup plus rapide que les résines polyesters ou vinyl-ester. Également, le système d'injection à haut débit SRIM permet de remplir le moule plus rapidement. L'utilisation d'un tel système permet d'augmenter le volume de production des pièces composites, par contre il est plus coûteux que le RTM car il requiert des moules avec de meilleures propriétés mécaniques.

La première partie de cet ouvrage est consacrée à l'étude des procédés RTM et SRIM dans la fabrication de pièces composites à coeur de mousse. Le coeur de mousse a pour fonction de conserver la stabilité dimensionnelle de la préforme en fibre de verre et son épaisseur durant l'injection de la résine. Le problème occasionné principalement par l'injection haut débit SRIM est la compression et le déplacement du coeur de mousse. La compaction du coeur de mousse occasionnera des points faibles dans la pièce telle une distribution non-homogène de la résine dans l'épaisseur du laminé ainsi que des zones sèches dans le renfort. Le renfort étant comprimé durant l'injection, il y aura une variation locale du taux de fibre et donc de la perméabilité. Dans ce cas précis, la loi de Darcy linéaire n'est pas applicable. Pour étudier ces conditions de moulage, des expérimentation ont été effectué sur deux types de moules, l'un étant un moule plaque carré et l'autre étant un moule à section quasi-rectangulaire. Des coeurs de mousse à densités variables ont été utilisés dans

chacun des moules. Le premier comprenait des mats de fibre de verre aléatoire continu déposé sur une plaque de mousse et le second un des fibres de verre tissés autour d'un noyau de mousse. La compaction du renfort et la déformation du coeur de mousse a été mesuré dans les deux cas.

La deuxième partie de cet ouvrage est consacré à l'étude du procédé CRTM (Compression Resin Transfer Molding) et de ses variantes possibles. Le CRTM a pour but d'obtenir une pièce composite possédant une plus grande concentration de fibre que la traditionnelle injection RTM (Resin Transfer Molding). Le procédé consiste à placer une préforme de fibre de verre dans un moule dont les cavités sont gardées partiellement ouvertes. L'ouverture des cavités permet d'injecter la résine plus facilement, car les renforts offrent moins de restriction qu'un moule fermé. Tout de suite après l'injection, le moule est fermé forçant la résine à entièrement mouiller les fibres. Deux types d'expérimentations ont été pratiqués. La première consiste à utiliser une préforme de tissu de verre thermoformée à l'épaisseur finale de la pièce. Celle-ci est déposée dans un moule plaque rectangulaire légèrement ouvert. La résine est injectée dans le canal vide entre la paroi supérieure du moule et la surface de la préforme. Le moule est par la suite fermé permettant de mouiller uniformément la préforme. La seconde expérimentation utilise des mats de fibre de verre aléatoire continu remplissant complètement une cavité de moule légèrement entrouverte. Lors de l'injection, la résine imbibe graduellement le

renfort à travers son épaisseur. La nouvelle approche est d'injecter la résine en même temps que le moule est fermé. Cette méthode expérimentale s'apparente à la déformation des coeurs de mousse et à la compaction des renforts discuté au Chapitre 2 du présent ouvrage. Dans les deux cas, nous sommes en présence d'une loi de Darcy avec une perméabilité non-linéaire.

CHAPITRE 1

REVUE DE LA LITTÉRATURE

Les travaux traitant de la compression de coeur de mousse lors du moulage utilisant le procédé RTM ou SRIM, et ceux traitant de la fermeture séquentielle d'un moule selon le procédé RTM sont pratiquement inexistants. Par conséquent, la littérature traitera des principes fondamentaux de la compressibilité des renforts, de la perméabilité et de l'écoulement des fluides selon la loi de Darcy.

1.1 ÉCOULEMENT DES FLUIDES EN MILIEU POREUX SELON LA LOI DE DARCY

L'écoulement des fluides en milieu poreux a été étudié dans divers domaines tels l'eau des nappes phréatiques, les filtres et la fabrication du papier par pressage. Plusieurs articles traitant du sujet ont été publiés par Muskat (1937), Scheidegger (1957), Happel et Brenner (1965), Philip (1970) et Dullien (1979) [1]. La théorie de l'écoulement laminaire d'un fluide à travers un milieu homogène poreux est basé sur les études expérimentales développées par H. Darcy [2]. Ses études ont conduit à développer la loi de Darcy exprimant la relation entre la vitesse de l'écoulement V (m/s) et le gradient de pression $\Delta P_f/\Delta L$ (Pa/m) :

$$V = -\frac{k}{\mu}\frac{\Delta P_f}{\Delta L} \tag{1.1}$$

où k est la perméabilité planaire des renforts (m^2), μ la viscosité dynamique du fluide newtonien (Pa.s). La loi de Darcy est communément utilisée afin de mesurer la perméabilité des renforts dans le domaine des composites. Par contre, cette loi ne peut être utilisée afin de définir un comportement non-linéaire dans l'écoulement d'un renfort sous l'action d'une compression.

Selon la définition de la loi généralisée de Darcy, on constate que celle-ci possède un domaine de validité limité [3]. La loi de Darcy n'est considérée valide que pour des nombres de Reynolds définis dans un milieu poreux plus petit que 1 [4]. Le nombre de Reynolds Re_k dépendant de la perméabilité du milieu poreux peut-être défini ainsi :

$$\mathrm{Re}_k = \frac{V\sqrt{k}}{\nu} \tag{1.2}$$

où ν est la viscosité dynamique du fluide (m^2/s), k la perméabilité (m^2) et V la vitesse d'écoulement du fluide (m/s). De cette loi, on retient trois régimes d'écoulement: le régime Darcien ($Re_k < 1$), le régime transitoire ($1 < Re_k < 100$) et le régime turbulent ($Re_k > 100$). La loi de Darcy étant originalement développée pour l'écoulement d'un fluide newtonien, il est possible de l'adapter pour des modèles d'écoulement non-newtonien [5].

Certains auteurs remettent en question l'utilisation de la loi généralisée de Darcy pour l'injection de pièces composites avec renforts. Initialement développée pour des milieux poreux composés de sphères, elle est plus ou moins bien adaptée pour l'écoulement d'un fluide dans un milieu fibreux (fibres de sections cylindriques) ainsi que dans un moule (effet de bord au niveau des parois du moule). R.S. Parnas et Al. (1991) [6] divisent l'écoulement de la résine dans un renfort selon deux niveaux: macroscopique pour l'ensemble du milieu et microscopique au niveau local des fibres. Les vitesses du premier écoulement sont plus rapides que celles au niveau des fibres. Il est donc nécessaire de distinguer la perméabilité en milieu sec de celle en milieu saturée en résine, celle-là étant 20% supérieure à la seconde.

1.2 LA PERMÉABILITÉ DES RENFORTS

Dans le domaine des composites, la perméabilité caractérise la facilité avec laquelle la résine mouille un renfort de fibres à une pression donnée. Un matériau composite est toujours exprimé en fonction du pourcentage du volume de fibre (V_f) présent dans le laminé. On peut également définir la porosité d'un renfort comme étant le pourcentage de vide pour une épaisseur donnée.

La variation de la perméabilité avec le taux de fibre d'un renfort est généralement associée à l'équation de Kozeny-Carman :

$$K = \frac{R_f^2}{4K_z} \frac{(1-V_F)^3}{V_f^2} \tag{1.3}$$

où K_z est la constante de Kozeny, V_f le taux de fibre et R_z le rayon moyen des fibres (m). Le perméabilité prédite par cette équation est isotropique, n'étant pas valable pour des renforts unidirectionnels ou anisotropes.

Gutowski et Al. [7] ont proposé un modèle modifié pour les renforts unidirectionnels pour différentes constantes de Kozeny dans différentes directions. Gutowski et Al. [8] ont proposé le modèle suivant :

$$K = \frac{R_f^2}{4K'} \frac{\left(\sqrt{\frac{V'_a}{V_f}} - 1\right)^3}{\left(\frac{V'_a}{V_f} + 1\right)} \tag{1.4}$$

où V'_a et K' sont des paramètres empiriques. Mais la faiblesse de ces équations dans le domaine des composites est quelles ne sont couplées à la géométrie des renforts que par le rayon des fibres R_f.

Deux méthodes existent pour mesurer la perméabilité d'un renfort, soit selon un écoulement directionnel ou selon un écoulement bidirectionnel pour une pression d'injection constante ou un débit constant. Adams et Al. (1986-1988) ont utilisé la technique de mesure de perméabilité bidirectionnelle. Ils ont développé l'équation pour un écoulement isotrope et anisotrope.

1.3 LA COMPACTION DES RENFORTS

La compaction des couches d'un renfort consiste à la fermeture d'un moule sous une certaine pression afin de comprimer l'espacement entre les fibres. Les renforts peuvent également être comprimés lors de l'injection de la résine dans une cavité (Figure 1.1). Plusieurs articles traitent de l'effet de la compaction sur les renforts lors de la fermeture d'un moule mais il y a peu de littératures disponibles sur la compaction lors de l'injection de résine dans un moule.

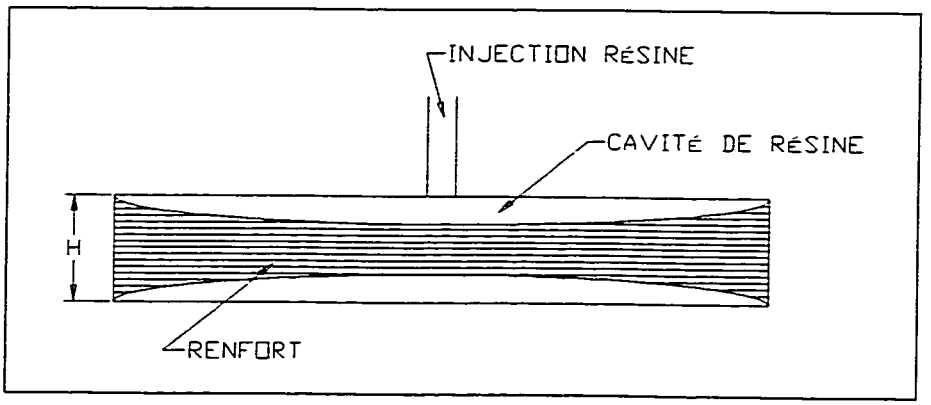

Figure 1.1 Compaction d'un renfort lors de l'injection de résine

K. Han et Al. [9,10] proposent une déformation d'un renfort basé sur la théorie des poutres. La déformation du renfort sera exprimée comme étant la flèche maximale de déformation d'une poutre soumise à une pression donnée.

T.G Gutowski [11] détermine également la compressibilité d'un renfort à l'aide de la théorie des poutres. T.G. Gutowsky et Al. [12] proposent un modèle semi-empirique du comportement de la rigidité des fibres confinés dans un espace restreint agissant comme des éléments poutres entre différents supports de contact :

$$P = A_S \frac{\sqrt{\frac{V_f}{V_o}} - 1}{\left[\sqrt{\frac{V_m}{V_f}} - 1\right]^4} \tag{1.5}$$

où V_f est le taux de fibre actuel, V_o le taux de fibre original et V_m le taux de fibre maximal. A_s est une constante d'élasticité dépendant de la séquence d'empilement et des propriétés des fibres :

$$A_s = \frac{3\pi E}{\beta^4} \tag{1.6}$$

où E est le module de flexion des fibres et β le rapport de la longueur sur la hauteur des fibres entre appuis définissant leurs rigidité.

Jönsson et Jönsson [13,14] étudient l'écoulement d'un fluide dans un milieu poreux compressible. Le comportement sous conditions stationnaires et dynamiques est analysé. Ils définissent une expression afin de déterminer la compressibilité d'un renfort selon une équation d'écoulement SSF (Steady-State Flow Equation). Une approche numérique est développée pour l'écoulement transverse dans un renfort.

Bakalémian et Hammani [15] ont travaillé à développer une méthode pour calculer la déformation d'un renfort subi lors de l'injection de résine basée sur la théorie des plaques. Une variation parabolique de la pression a été utilisée afin d'exprimer la flèche maximale de déformation du renfort :

$$w(x,y)=\sum_{m=1,2,3}^{\infty}\sum_{n=1,2,3}^{\infty}\left\{\frac{P_{mn}\sin\left(\frac{m\pi x}{a}\right)\sin\left(\frac{n\pi y}{b}\right)}{D\pi^4\left(\left(\frac{m}{a}\right)^2+\left(\frac{n}{b}\right)^2\right)^2+k}\right\} \tag{1.7}$$

où w représente la flèche (m), P_{mn} le type de distribution de pression (variation parabolique dans notre cas), a et b la dimension de la plaque (m) et k la pente de compressibilité du renfort (Pa/m). La rigidité en flexion du fibre est exprimée par:

$$D=\frac{Eh^3}{12\left(1-\gamma^{2)}\right)} \tag{1.8}$$

où E est le module de flexion de la fibre (Pa), h l'épaisseur du renfort (m) et γ le coefficient de poisson.

1.4 REMPLISSAGE D'UN MOULE SELON LES PROCÉDÉS RTM ET SRIM

Généralement le but ultime des études traitant des procédés de moulage LCM (Liquid Composite Molding) consistent à prédire la position du front d'écoulement de la résine à tout instant du remplissage, les gradients de pressions à l'intérieur du moule ainsi que les vitesses de remplissage. Un design

optimal du moule permettra de bien positionner l'injection de la résine, de distribuer uniformément la pression dans la cavité ainsi que de déterminer l'emplacement et le nombre des bouches d'évacuation d'air.

Divers logiciels de simulations ont été créés pour prédire le remplissage de couches de renfort d'une préforme en fibre de verre. La loi de Darcy est utilisée pour prédire l'écoulement du fluide dans le renfort. Le logiciel RTMFLOT [16] permet de prédire un tel remplissage pour des pièces RTM. Il permet de simuler et de visualiser la phase de remplissage d'un moule pour des conditions isothermes ou non-isothermes.

PRÉSENTATION DU CHAPITRE 2

Le chapitre 2 est consacré à l'étude des procédés RTM et SRIM dans la fabrication de pièces composites à coeur de mousse. Le coeur de mousse a pour fonction de conserver la stabilité dimensionnelle de la préforme en fibre de verre et son épaisseur durant l'injection de la résine. Le procédé RTM est avantageux pour fabriquer de telles pièces en coeur de mousse, car l'injection à basse pression (5-10 bar) requiert un équipement peu coûteux en terme de moule et d'équipement d'injection. Comparativement au RTM, le procédé SRIM produira des montées de pression beaucoup plus élevées dans les moules.

Le principal problème occasionné par l'injection SRIM est la compression et le déplacement des coeurs de mousse. Une distribution non-homogène de la résine au niveau de l'épaisseur causera des points faibles dans la pièce. À cause du déplacement du coeur de mousse, il y aura une variation locale du taux de fibre et donc de la perméabilité. Dans ce cas précis, la loi de Darcy linéaire n'est pas applicable. Les expérimentations ont été effectuées sur deux types de moules, l'un étant un moule plaque carré et l'autre étant un moule à section quasi rectangulaire. Des coeurs de mousse à densités variables ont été utilisés dans chacun des moules. Le premier comprenait des mats de fibre de verre aléatoire continu déposé sur une plaque de mousse et le second des fibres de

verre tissé autour d'un noyau de mousse. La compaction du renfort de verre et la déformation du coeur de mousse a été mesuré dans les deux cas.

CHAPITRE 2

EXPERIMENTAL ANALYSIS OF CORE CRUSHING AND CORE MOUVEMENT IN RTM AND SRIM FOAM CORED COMPOSITES PARTS

S. Wirth, École Polytechnique de Montréal, Qué., Canada
R. Gauvin, École Polytechnique de Montréal, Qué., Canada
K. N. Kendall, Ford Motor Company, Dearborn, Mi, USA

2.1 ABSTRACT

In liquid composite molding, SRIM can typically achieve a higher pressure than the RTM process. When molding a foam cored composite part at high flow rates using an SRIM system, the following related effects can be observe: high molding pressures, core shifting, core crushing, variable permeability and reinforcement compaction. Because of the variable permeability in such conditions, the linear Darcy law does not apply for flow simulation. Finally, all this can easily result in dry spots defects.

To study the various problems occurring in the molding of foam cored composite parts, two molds equipped with pressure transducers were used. The first one was a picture frame square plaque mold. To ease the measurement of reinforcement compaction and core crushing, flat panels were molded with reinforcement on one side only. The second part was a quasi rectangular foam cored beam with braided reinforcement all around the foam core. In this paper, it

is refers as the Small Core part. With this part, reinforcement compaction, core crushing and core shifting was measured.

The picture frame plaque mold was used with the RTM and SRIM processing equipment. Continuous strand mat with a constant fiber volume fraction was used with Polyurethane foam of variable density. For the RTM process, Vinyl Ester resin was injected at constant pressure while for SRIM, Polyurethane resin was injected at constant flow rate. Parts were cut to measure laminate thickness and core deformation. For the Small Core mold, only the SRIM system was used with a constant flow rate. In this case the core materials used were Polyurethane of various densities. All parts were braided with ±45° and axial (0°) glass filaments. For some parts, locators were placed on the core surface to prevent its shifting. Short shots were used to observe the resin flow progression.

For the picture frame experiments, the RTM process gave no significant core deformation. With the SRIM system, results showed a non-negligible core deformation at some foam densities. The SRIM system was also used with the Small Core tool. The results revealed the dominance of the core shifting and fabric compaction over core crushing. The use of locators placed on the core surface led to a better flow progression and nearly eliminated the core shifting, resulting in a part without defects. The flow simulation software RTMFLOT developed in our laboratory and based on a linear Darcy Law was used with

these complex cases. The simulations results gave a good approximation of the gate pressure during filling.

2.2 INTRODUCTION

The automotive industry is interested in LCM processes for weight reduction, part integration, time and cost savings. Resin Transfer Molding (RTM) and Structural Reaction Injection Molding (SRIM) are processes well suited for the manufacturing of composite components with lightweight cores. Same or higher properties than steel or aluminum parts can be achieved using skinned composite parts. The core function is to retain the preform and keep dimensional shape and thickness during the resin injection. The RTM process can be adequately used for foam cored composite parts because low cost molds and machines can be used due to the low injection pressure range, 5 to 10 bar. Typically, SRIM will give higher pressures then RTM meaning more expensive molds. Also, more costly investments must be made for SRIM systems. However, highly reactive Polyurethane and high flow rates (100-400g/sec) will give faster production rates than RTM and justify in several applications the choice or SRIM.

One of the concerns when using SRIM to mold foam cored composite parts is the core crushing. Core compression results in skins with non-homogenous resin distribution. For instance, higher resin fraction near the

injection port may result in structural weak points. SRIM high resin flow rates and pressure may deform or shift the core, creating a variable flow channel thickness. The core shifting can lead to dry spots in the part. Because of the reinforcement compaction, the fiber volume fraction and the permeability will vary with pressure. In that case, the linear Darcy's law currently use in LCM process models is no longer valid. To study these complex molding conditions, this paper presents the results of a series of experiments conducted with two molds especially design for foam cored composite parts. The first one is a picture frame square plaque mold. To ease the measurement of reinforcement compaction and core crushing, flat panels were molded with reinforcement on one side only. In the second mold, a quasi rectangular foam cored beam is molded. It used braided reinforcement slide over the foam core. In this paper is referred as the Small Core part. With both installations, reinforcement compaction and core crushing has been measured. Core shifting was also measured in the Small Core mold.

The flow simulation software RTMFLOT, developed in our laboratory and based on a linear Darcy's Law is also used to compare its predictions with the experimental results. The usefulness of this type of software, based on a linear Darcy's law, is evaluated in this complex case.

2.3 MATERIAL AND EQUIPMENT

2.3.1 Molding facilities

Figure 2.1 shows the schematic of the plaque molded in a steel picture frame cavity. An open channel of 9.5mm provided a line gate injection and 5 pressure transducers were located on the bottom part as show in Figure 2.1. As illustrated, all plaques were molded with the reinforcement on the bottom side only, facing the pressure transducers. In all cases, 6 layers of a continuous strand mat, the Unifilo U750-450 from Vetrotex was used. The composite skin thickness before molding was 6.4mm, giving a fiber volume fraction V_f = 22%. RTM and SRIM injection units were used with the plaque mold. Figures 2.2 and 2.3 shows the Small Core mold and part. It is a quasi rectangular cavity fitted with 17 pressure transducers (P1 to P17), located on the top, the bottom and on one side of the cavity. Parts were injected through a line gate located on the side and slightly offset with respect to the mold center line, as show in Figures 2.2 and 2.3. Only SRIM injection equipment were used with that mold.

2.3.2 Foam core properties

Polyurethane foam cores, the plaque and the rectangular core, were molded in epoxy tools with a two parts chemical system, isocyanate and polyol. For the low density range, 0.08 to 0.22 gr/cm^3, material supply by BASF was used in a ratio of 1.29 to 1. For higher density range, 0.32 to 0.38 gr/cm^3, an ICI formulation in a ratio of 1.49 :1 was used. In all cases, the density was varied by

changing the machine flow rate. For the plaque, thick blocks were molded in a cycle time of 20 minutes and then cut to the required 19mm thickness. For the Small Core, a cycle time of 10 minutes was enough.

Foam properties in compression were measured. Figure 2.4 shows the applied pressure versus deformation curves obtained at 80°C for the low density foam used. The curves are divided in three zones. As shown in Figure 2.4 for the 0.09 gr/cm^3 foam density, compression modulus E_1 and E_2 were derived from the first two zones. The last zone represents a plastic deformation. The values of these two compression modulus are given in Table 2.1. The tests were run at 80°C to obtain the foam behavior at the composite part molding temperature.

2.3.3 Resin and reinforcement

The properties and the supplier for the Vinyl Ester and Polyurethane resins used for the composite moldings are given in Table 2.2. For the plaque molding, 6 layers of a continuous strand random glass mat from Vetrotex, the Unifilo U750-450, was used. For the Small Core part, braided glass at ±45/0° was utilized. Figure 2.5 shows a schematic of the braiding process. Figure 2.6 shows the foam core and the braided reinforcement covering the core on the top and bottom section of the figure respectively. On the core picture, small thin parts glued on the surface can be seen. Later called « locators », these are design to prevent core shifting under resin pressure. Compaction data for the

reinforcements was measured. The results for the mat as well as for the braided material are shown in Figure 2.7. It gives the pressure versus the fiber volume fraction. These compaction tests were done between two steel plates fitted to a MTS hydraulic machine. Six layers of mat and three layers of braided material were used for these tests. Looking at the results, we notice that the braided material is easier to compact at the beginning but become stiffer after. As expected the fiber volume fraction of the glass mat is always much lower than the braided reinforcement. Finally, various data concerning these two reinforcements are given in Table 2.3.

2.4 EXPERIMENTAL

2.4.1 Plaque molding

A polyurethane foam density range of 0.08 to 0.14 gr/cm^3, was used for these experiments. A pressure pot with a constant injection pressure of 5 bar was used for RTM. As shown on Figure 2.1, the resin filled only the side where the glass mat was located. A fast gel time Ashland Vinyl Ester Resin was utilized to minimize the core relaxation after the injection. The resin properties are describe in Table 2.2. The resin at room temperature was injected in the mold heated at 65°C. The total cycle time was 10 minutes for a part fill time of about 30 seconds. The average flow rate and flow front speed were respectively 18 gr/sec and 1 cm/sec. Because of the RTM typical low pressure, these experiments gave no significant core deformation.

ICI Polyurethane resin was injected at a constant flow rate of 400 gr/sec. A sealant was placed all around the foam core edges to prevent resin overflow. The maximums in-mold pressures were between 5 to 6 bar for a flow front speed of 22 cm/sec. Room temperature resin was injected in a mold heated at 80°C giving a resin gel time less than 5 second. The injection time was chosen to precisely stop the resin flow before it reached the vents. With this precaution, the final foam compaction should be roughly the same than the one occurring during the molding of a production part.

Each molded plaque was cut in half along the pressure transducer centerline shown in Figure 2.1 and the core thickness measured at the five transducer locations. Because of the in-mold pressure, the foam core elastic relaxation gives a larger overall part thickness than the in-mold thickness. To calculate the in-mold core thickness, the 25.4mm mold cavity height was taken as the constant part thickness. The upper section of Figure 2.8 illustrates the plaque measurements before and after molding. In some cases, even with the sealant, the resin ran between the upper mold cavity and the foam plaque core as illustrated on the figure, with « F » indicating the top flow thickness. The final core thickness was calculated as follow :

$$C_f = M_i - (L + F) \qquad (1)$$

and the core deformation as the final core thickness minus the initial core thickness at zero pressure with the expression :

$$D_c = C_f - C_i \qquad (2)$$

2.4.2 Small Core molding

Polyurethane foam density range, 0.12 to 0.38 gr/cm^3, was used for these experiments. With SRIM set-up, ICI Polyurethane resin was injected at a constant flow rate of 150 gr/sec giving an approximate flow front speed of 3 cm/sec. The part fill time was around 2.5 seconds. The results revealed the dominance of the core shifting and fabric compaction over core crushing. Due to the resin high flow rate, the Polyurethane foam core was crushed and shifted on the opposite side of the line gate leading to dry spots in the composite shell. The fabric being compacted by the core, the increased in glass volume fraction locally, result in a lower permeability. To completely filled up the part, it was essential to eliminate the core shifting. To overcome this problem, thin wood inserts were placed between the foam core and the braided material to minimize the core shifting during the injection. The upper section of Figure 2.6 shows wood locators glued on the top, bottom to and sides of the core. The positions of the 2mm thick locators were chosen for optimum part filling. The locators almost canceled the core shifting but in some cases the foam was slightly penetrated by the wood inserts. The short shots illustrated in Figure 2.9 clearly shows the benefit of using locators. It demonstrates that a complete part filling was impossible (Fig. 2.9 left side) without using wood inserts on the core surface (Fig. 2.9 right side).

The composite Small Core was cut in six pieces along the top and bottom pressure transducer positions for laminate and core measurements. The bottom section of Figure 2.8 shows a schematic of a cut core section before and after molding. The foam core deformation in the X and Y direction was calculated as follow :

$$D_cx = (Lx_1 + Lx_2) - 2L_{init} \quad (3)$$

$$D_cy = (Ly_1 + Ly_2) - 2L_{init} \quad (4)$$

and the core shifting at is center point was measured with these equations :

$$Mx = |Lx_1 - Lx_2| \quad (5)$$

$$My = |Ly_1 - Ly_2| \quad (6)$$

The foam core deformation D_cx, D_cy and the core displacement Mx, My were calculated using average values of the six core sections.

2.5 RESULTS AND DISCUSSION

2.5.1 Plaque mold

For a constant resin injection flow rate of 400 gr/sec, the maximum in mold pressure was fluctuating between 5 and 6 bar. To be sure to correlate the injection pressure with the foam compaction, it was necessary to end the resin injection before a pressure build up. Figure 2.10 shows a typical pressure distribution versus time plot for each pressure transducer for a test with a low foam density. The pressure curves do not end with the same maximum pressure

because the injection was stopped when the flow front reached the fifth pressure transducer (P5).

As shown in Figure 2.11, the maximum pressure at the line gate seems to rise linearly with the foam core density. The pressure will be lower for a low foam density because it deforms more, leading to a higher permeability in the skin. When the core density increase, the core deformation is reduced and the reinforcement permeability is smaller. Figure 2.12 illustrates the foam core compaction versus its density, at two different locations. The scattering of the results is important, especially at location P1. Nevertheless, a power law of order 2 is used in Figure 2.12 to illustrate the relationship. Because the maximum pressure at the line gate can be higher than the compression modulus of low density foam, this can result in a large core compaction, leading to a non-linear relation.

To evaluate how the foam compaction tests run at 80°C could be used to predict the foam core crushing during the injection process, Figures 2.13, 2.14 and 2.15 are presented. In these figures, the core compaction during filling, as measured at each pressure transducer location, is reported for ten experiments run with various core densities. In these figures, the dotted line ties the compaction value of the core, as measured at 80°C, for the average pressure value taken from the experiment at each pressure transducer location. The

experimental data used in Figures 2.13, 2.14 and 2.15 are given in Table 2.4. As shown in Figure 2.13, the intervals between the data points from moldings are large for the same location and do not follow very well the compression test. On the other hand, for the higher foam densities illustrated in Figure 2.14 and 2.15, the experimental results are more predicable from compression test curves. Also, the scattering in the data points from molding is reduced. In all cases however, the foam compaction at the line gate location can not be predicted accurately with the values from the compression tests. In all of these three figures the measured value during molding is lower then the value from the compression curves. One reason might be the fact that the bi-directional pressure distribution at the edge of the foam at the line gate influences the foam compaction behavior.

2.5.2 Small Core mold

A maximum gate pressure of 5 to 35 bar was observed depending on the foam density for a constant 150 gr/sec injection flow rate. The foam core compaction results in the X and Y directions were calculated with equations 3 and 4 respectively divided by the foam core thickness. Table 2.5 shows the non-dimensional foam core compaction (mm/mm) for each direction calculated for the Small Core foam without wood locators. The results show similar compaction for each direction.

The core shifting measurements for foam surfaces with and without wood locators in the X and Y directions were compared in Figures 2.16 and 2.17 respectively. The histograms, representing the core shifting versus the foam density from Tables 2.5 and 2.6, showed the benefit of using wood locators. One can see that the core shifting was greatly reduced by the wood locators.

The laminate thickness of the Small Core « L » (see Fig. 2.8) has been approximated with compression test results on the braided fabric. As shown in Table 2.5, only the minimum laminate thickness was kept at the maximum in-mold pressure. The same maximum in-mold pressure was used to evaluate the braid thickness from the compression tests. It can be observe from Table 2.5 that the laminate thickness from the experimental values are larger then the values from the compression tests. The results show that the braid compression can not be well approximated with a compression test. The in-mold situation is more complex because many parameters should be analyzed such as the resin injection rate, the line gate location and dimension, the foam shape, the foam density and shifting.

Table 2.7 represents the Small Core final part and resin weight for all foam densities. Also, the percentage of resin in each part was calculated. For low foam densities, the amount of resin is higher because of the core crushing. Since the part price is function of the resin volume, a part with a low density foam

will be more expensive than a one piece with a high density foam. The part weights seems to be relatively constant for the low foam density range, from 0.12 to 0.20 gr/cm^3. At higher densities the foam core will not be crushed, so the resin volume will remain constant and the part weight will rise with the foam weight increase only.

2.5.3 Flow simulation of plaque mold

During the filling of a sandwich part, since the foam core is deformed under resin pressure, the laminate thickness varies and the permeability as well. A flow simulation should be with a modified Darcy's law, taking care of a variable permeability in function of time. However, most of the existing simulation software like RTMFLOT developed in our laboratory, are based on a linear Darcy's law. To evaluate the usefulness of such a software to predict the flow conditions in the actual non-linear case, simulation of the plaque molding experiments was done using our software RTMFLOT. The analysis was done for three foam density, 0.09, 0.11 and 0.13 gr./cm^3. For each experiment with a given foam density, the skin thickness at each pressure transducer location was measured. For the simulation, a continuously variable skin thickness was used, as shown in Figure 2.18. For each zone, the thickness of the simulation corresponds to the average measured value at each pressure transducer. Flow simulation in this variable skin thickness was done. The simulation parameters for each zone and for the three foam densities investigated are given in Table

2.8. The resin viscosity used was 20 mPa-sec. Figures 2.19, 2.20 and 2.21 show the measured and simulated gate pressure as a function of the filling time for 0.09, 0.11 and 0.13 gr./cm^3 foam density respectively. As can be observed, in all case, the simulation underestimates the experimental value, However, the results are reasonably good for the two higher densities.

2.6 CONCLUSION

The SRIM experiments with the plaque mold gave interesting results regarding core compaction. For low polyurethane foam densities, the core compaction during molding was not negligible. It was successfully compared with compression tests made on polyurethane foam, especially for higher foam densities. The pressure distribution was found to rise linearly with low foam density. The simulations with the RTMFLOT software using the linear Darcy's Law gave a good approximation of the gate pressure distribution.

The SRIM molding with the Small Core tool revealed the dominance of the core shifting and fabric compaction over core crushing. The wood locators used on the foam surface greatly reduced the core shifting and eliminated dry spots from fabric compaction. The minimum laminate thickness prediction at maximal in-mold pressure using the braid compression test data only gave approximate results. Finally, it was found that the lowest foam densities did not give necessarily the lightest or cheaper part.

2.7 ACKNOWLEDGMENTS

The authors would like to thank FCAR (Fonds pour la formation de chercheurs et l'aide à la recherche du Canada) for the financial support given to Mr. Stéphane Wirth, the National Science and Engineering Research Council of Canada for its financial assistance, the SRL (Scientific Research Laboratory) of the Ford Motor Company for the used of their assistance and their LCM facilities and APX Company for the used of their foam processing facilities. Also, he would like to thank the assistance of the following persons: Dr. Ken Kendall (Ford Motor Company) and Dr. Raymond Gauvin (École Polytechnique de Montréal).

2.8 REFERENCES

1. **GAUVIN, R. TROCHU, F.** (1994). « RTMFLOT, un logiciel intégré et modélisation des procédés RTM », *Composites,* ***5,*** 16-22.
2. **KENDALL, K.N. RUDD, C.D. OWEN, M.J. MIDDLETON, V.** (1992). « Characterization of the resin transfer moulding process », *Composites Manufacturing, **3**, 4*, 235-247.
3. **KENDALL, K.N.** (1994). « Component and Process Design for Liquid Composite Moulding », *Int. Conf. on design and manufacturing using Composites, ATNAM '94, Montreal.*
4. **FERLAND, P., GUITTARD, D., TROCHU, F.** (1996). « Concurrent methods for permeability measurement in resin transfer molding », *Polymer Composites, **17**, 1*, 149-158.

5. **C.F. JOHNSON, N.G. CHAVKA, R.A., JEYRON.** (1986). « Resin Transfer Moulding of Complex Automobile Structures », *Proceeding of 41st Annual Conf. of the Reinf. Plastics Comp. Inst., Society of the Plastics Industry Inc., session 12-A.*

6. **C.D. RUDD, E.V. RICE, L.J. BULMER, A.C. LONG.** (1993). « Process Modelling and Design for Resin Transfer Molding », *Plactic, Rubber and Composites Processing and Applications, **20**, 2,* 67-76.

7. **GAUVIN, R. and CHIBANI**, (1986). « The Modeling of Mold Filling in Resin Transfer Molding », *International Polymer Processing, **1**, 1,* 42-46.

8. **GAUVIN, R., TROCHU, F.** (1996). « Keys Issues in Numerical Simulation of Liquid Composites Molding Processes », *Proc. Of the 29th ISATA Conf.,* 1107-1114.

9. **TREVINO, L., LEE, L. J., RUPEL, K., LIOU, M. J.** (1990). « Permeability and compressibility measurement of fiber mats in resin transfer molding ands structural RIM », *45rd Annual Conf., Comp. Inst., Soc. Plas. Ind., Feb. 12-15.*

10. **W.B YOUND, K. HAN, L.H. FONG, L.J. LEE, M.J. LIOU.** (1991). « Flow Simulation in Molds with pre-placed Fiber Mats », *Polymer Composites, **12**, 6,* 391-403.

11. **GAUVIN, R. CLERK, P. LEMENN, Y. TROCHU, F.** (1994). « Compaction and Creep Behavior of Glass Reinforcement for LCM », *Proc. of the 10th Annual ASM/ESD Advanced Composites Conf.,* 357-367.

12. **D.A. BABBINGTON, J.H. ENOS, J.M. COX.** (1987). « High Speed RTM of Vinyl Ester Resins », *AUTOCOM-87, Dearborn, MI, EM87-351.*

13. **GAUVIN, R. AND CHIBANI, M.** (1988). « Modelization of the Clamping Force and Mould Filling in Resin Transfer Moulding », *43rd Annual Conference of the Composite Institute.*

2.9 NOMENCLATURE

A : Cross-sectional area (m^2)

C_f : Final core thickness

C_i : Initial core thickness at zero pressure (19.1mm)

D_c : Core deformation

D_cx : Core deformation in the x direction (width)

D_cy : Core deformation in the y direction (height)

$\delta p / \delta x$: Pressure gradient ($N\ m^{-1}$)

E1 : First compression modulus

E2 : Second compression modulus

F : Top flow thickness

K : Global permeability (m^2)

L : Laminate thickness

L_{init} : Initial laminate thickness in the mold cavity (4.5mm)

Lx_1 , Lx_2 : Laminate thickness in the x direction on both side of the core

Ly_1 , Ly_2 : Laminate thickness in the y direction on both side of the core

M_i :	Mold cavity thickness (25.4mm)
Mx :	Center core shifting in the x direction (width)
My :	Center core shifting in the y direction (height)
μ :	Viscosity (N s m^{-2})
P1 - P17 :	Pressure transducer
Q :	Volumetric flow rate (m^3 s^{-1})
T1 :	Thermocouple
Vf :	Glass fiber volume fraction

2.10 FIGURES

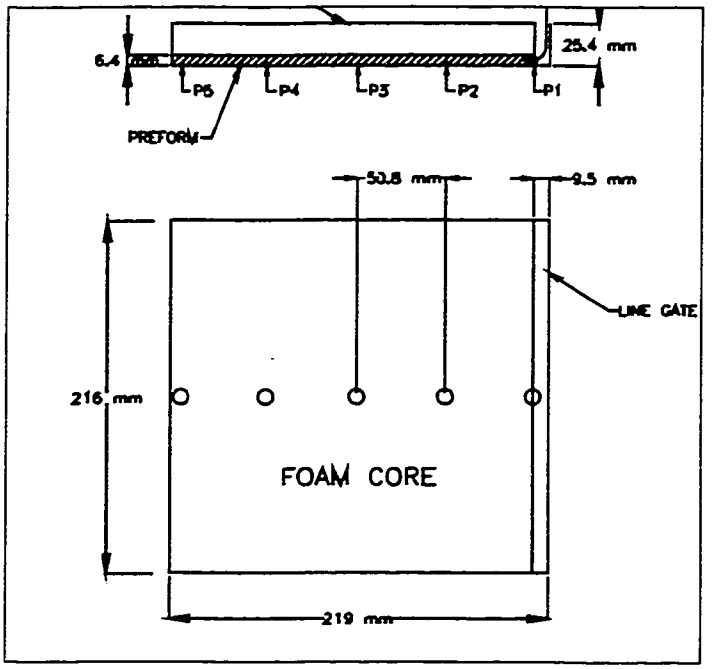

Figure 2.1 Schematic of the molded plaque and pressure transducer locations

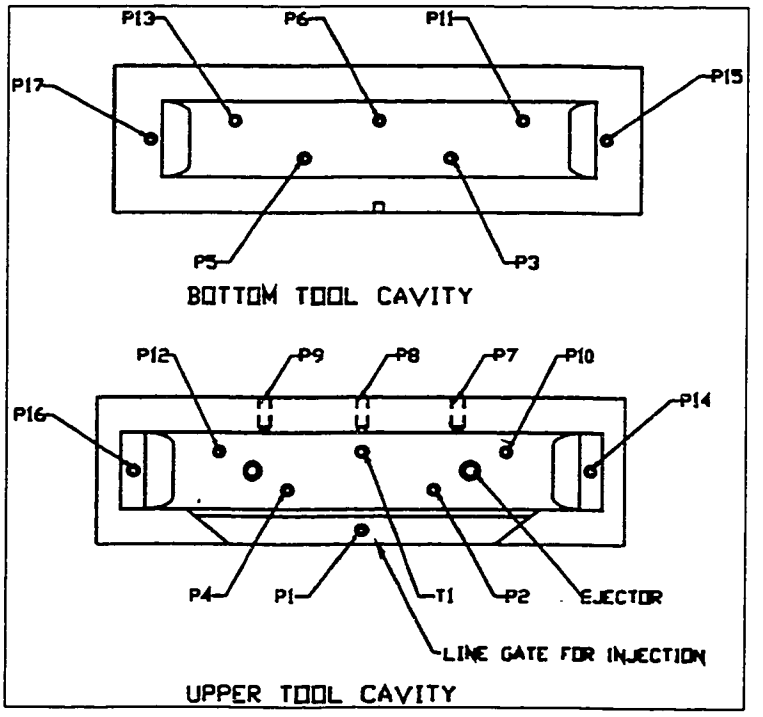

Figure 2.2 Small core tool dimensions

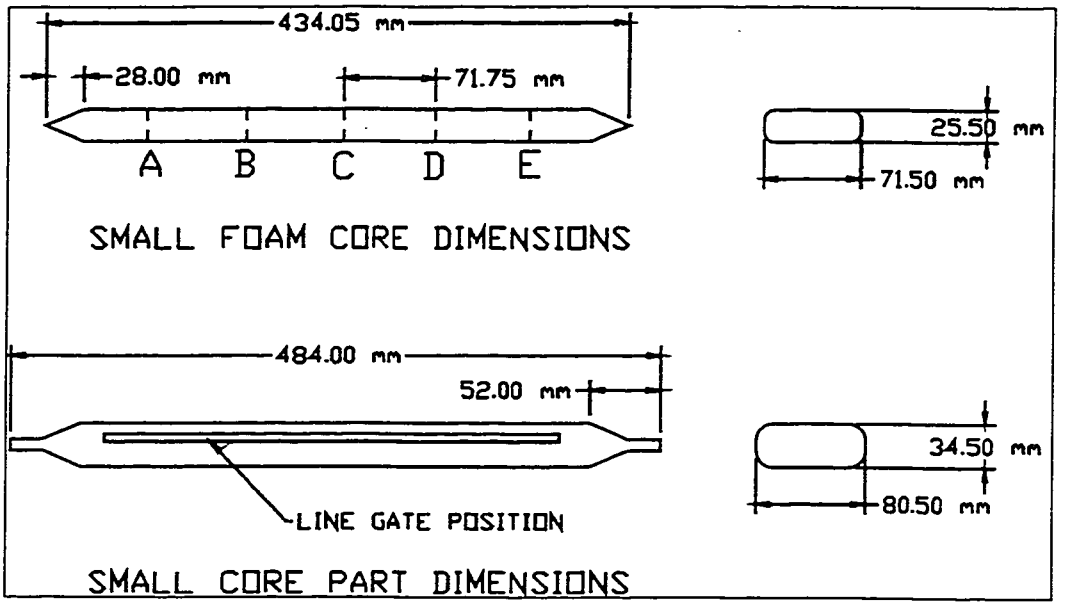

Figure 2.3 Small core part dimensions

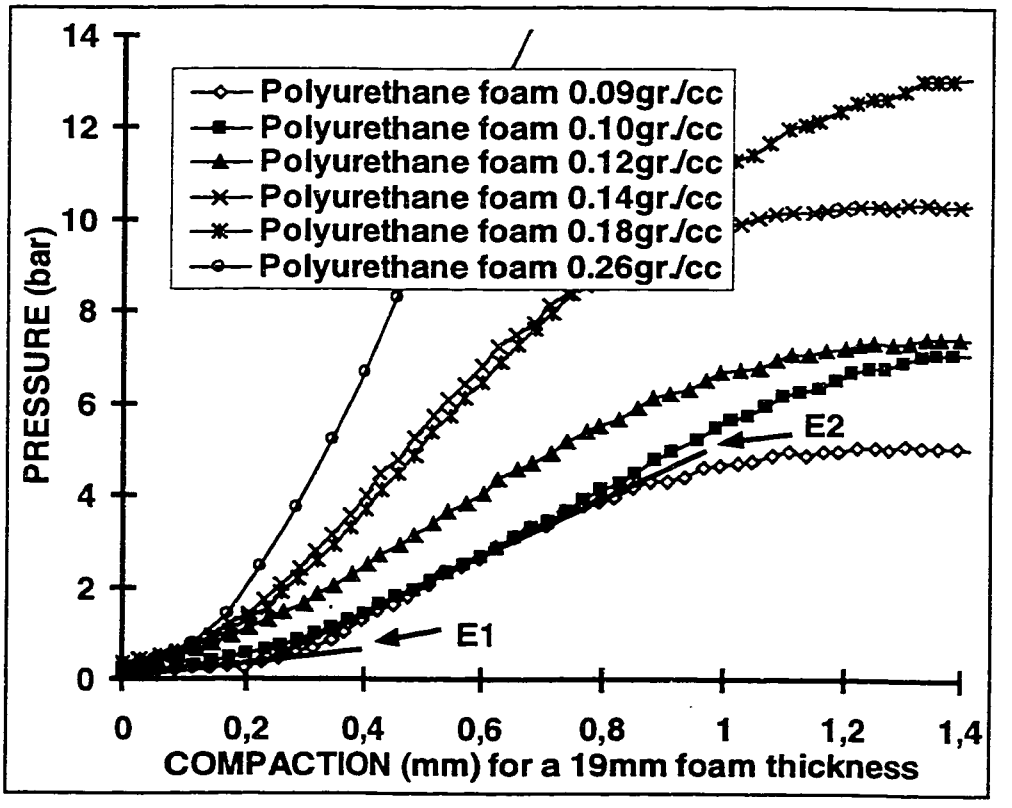

Figure 2.4 Compaction tests @ 80°C for polyurethane foam of variable densities

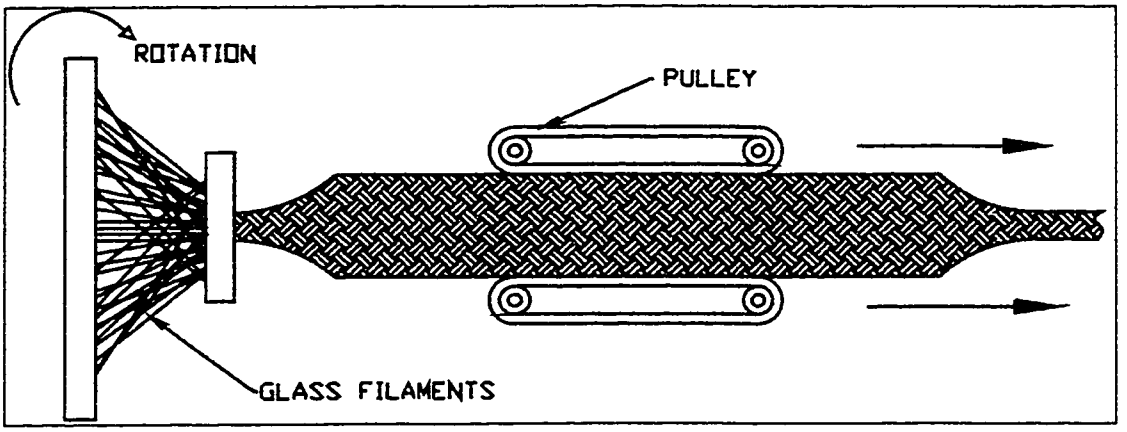

Figure 2.5 Braiding process

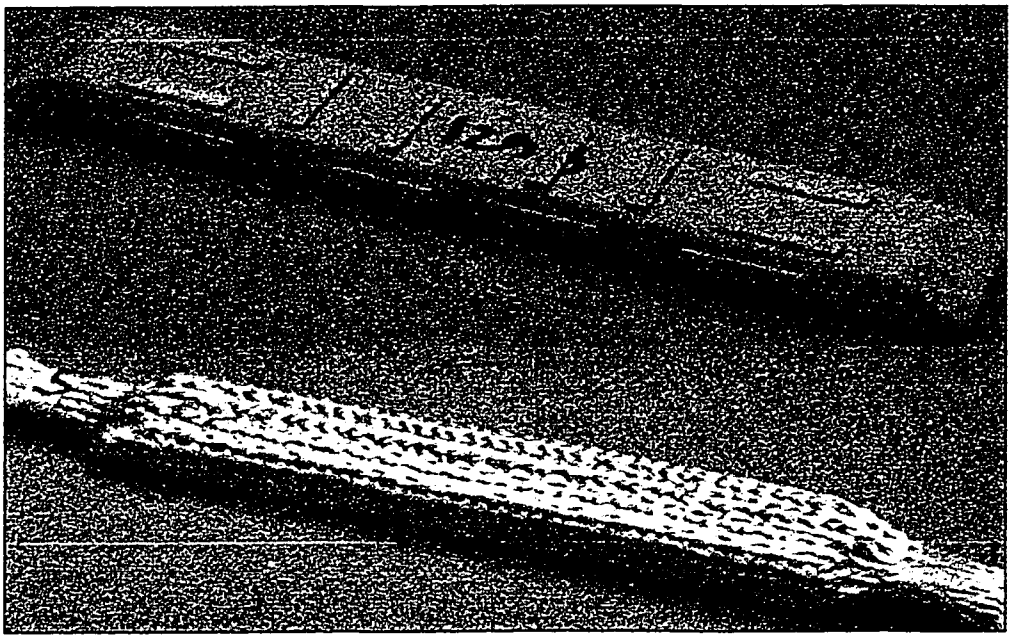

Figure 2.6 Polyurethane small core before and after braiding

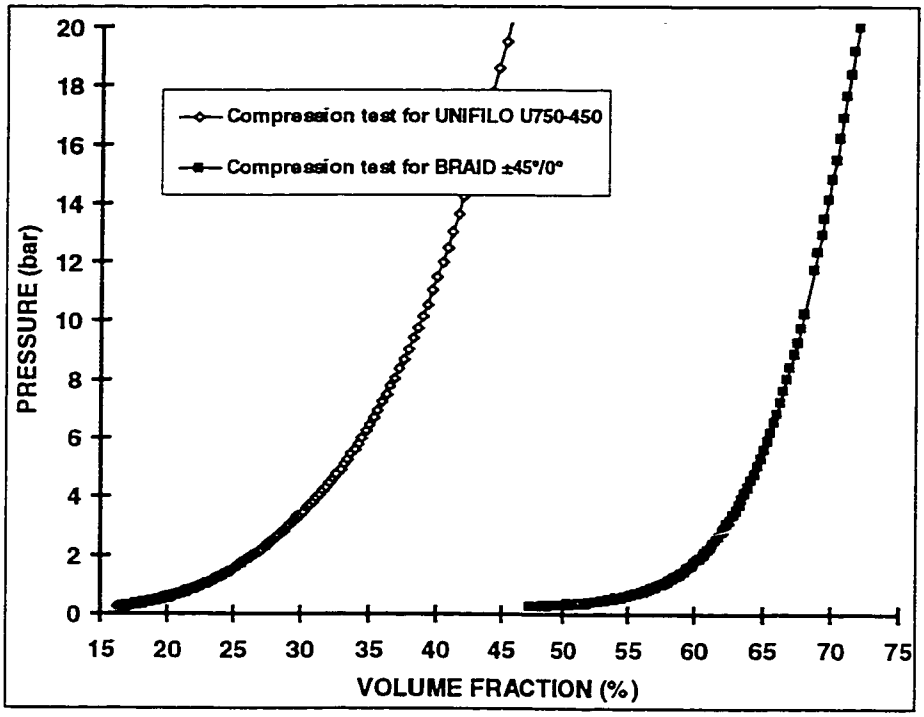

Figure 2.7 Compression tests with 6 layers of fabric for Unifilo (U750-450) and braided glass (±45°/0°)

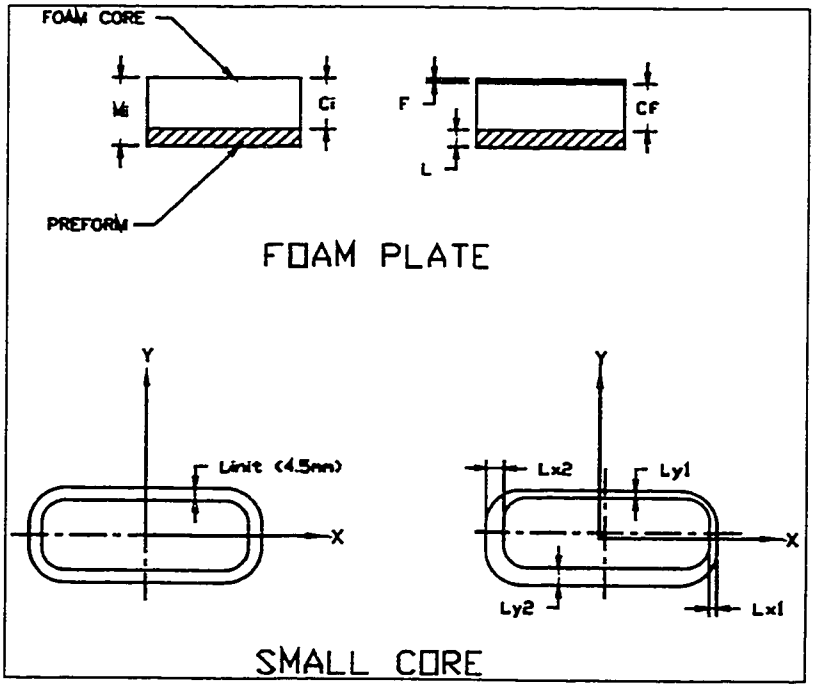

Figure 2.8 Plaque and small core part measurements

Figure 2.9 Small core short shots with (right) and without (left) wood locators

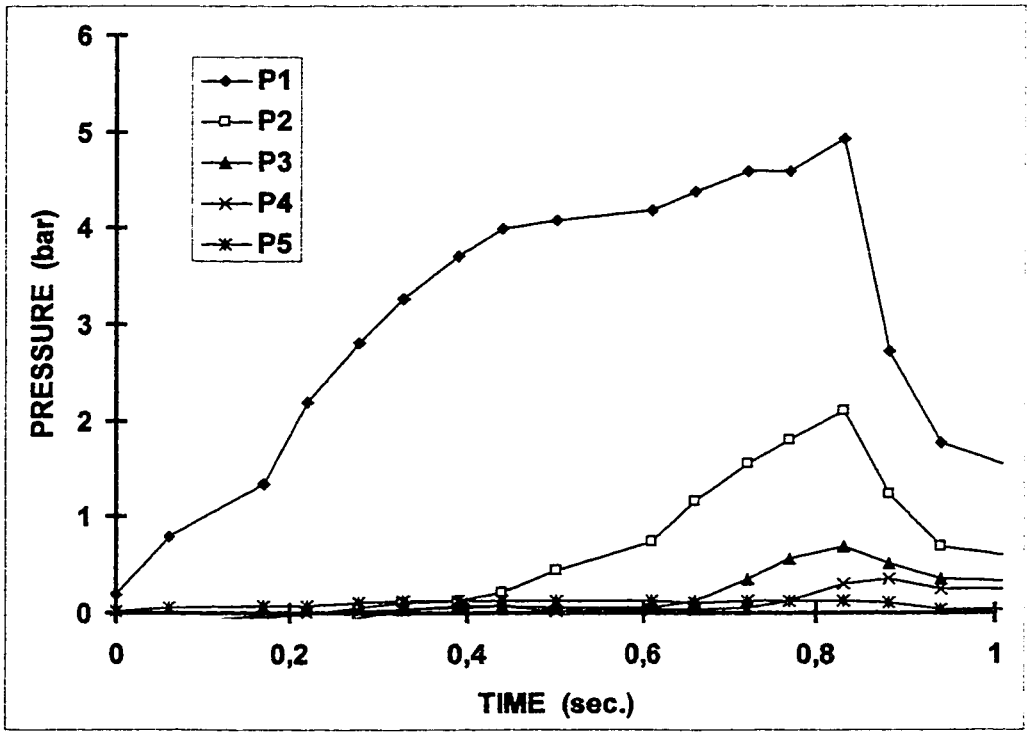

Figure 2.10 Typical pressure distribution for plaque mold
(Foam density = 0.09 gr./cc)

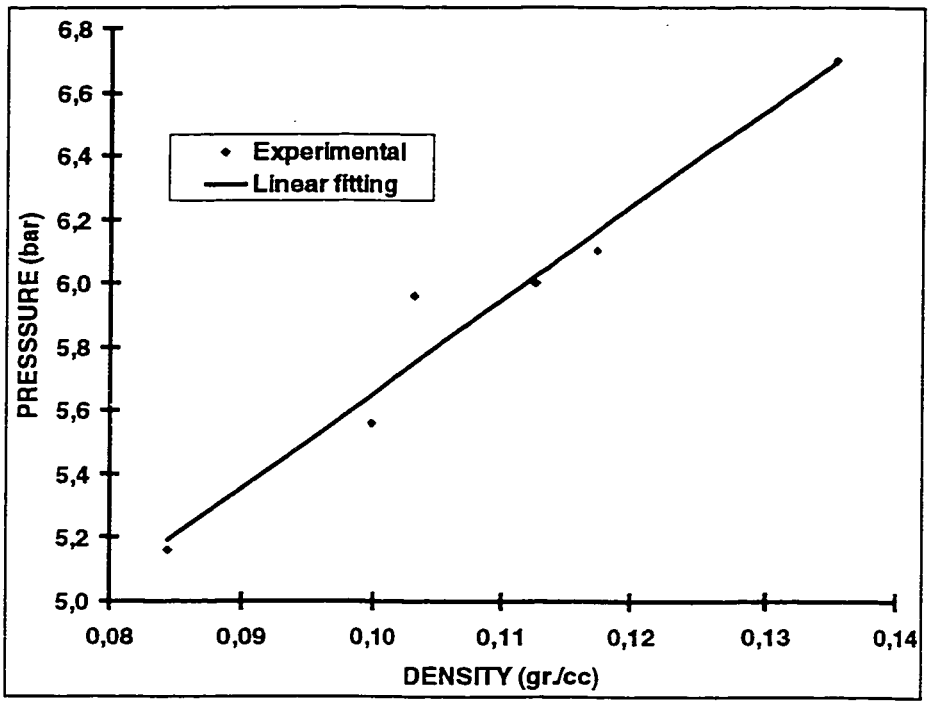

Figure 2.11 Plaque molding pressure at line gate for various polyurethane foam densities

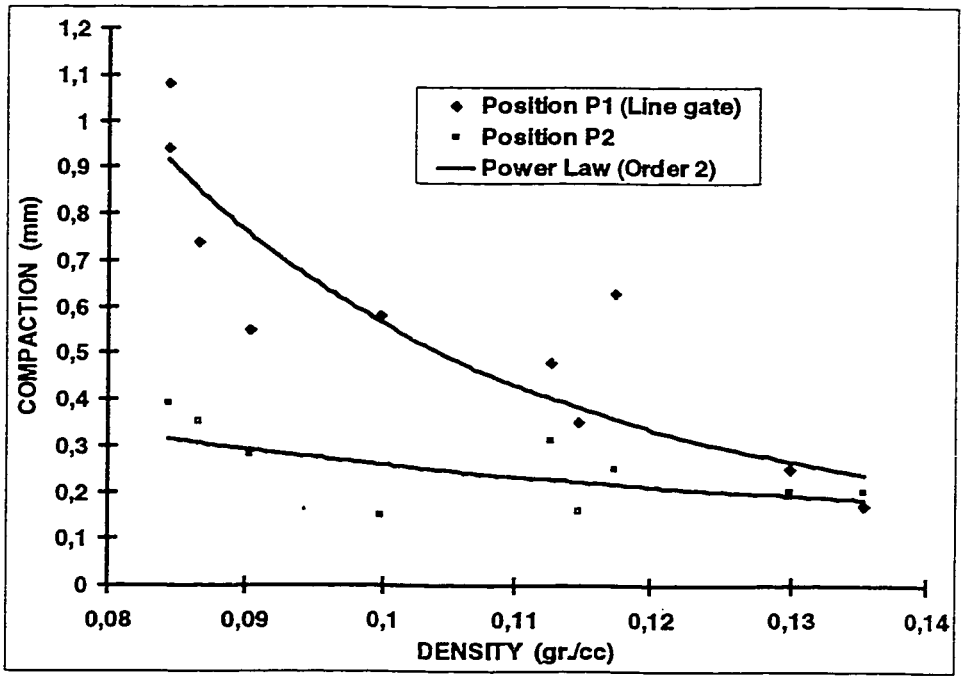

Figure 2.12 Plaque core compaction for various polyurethane foam densities

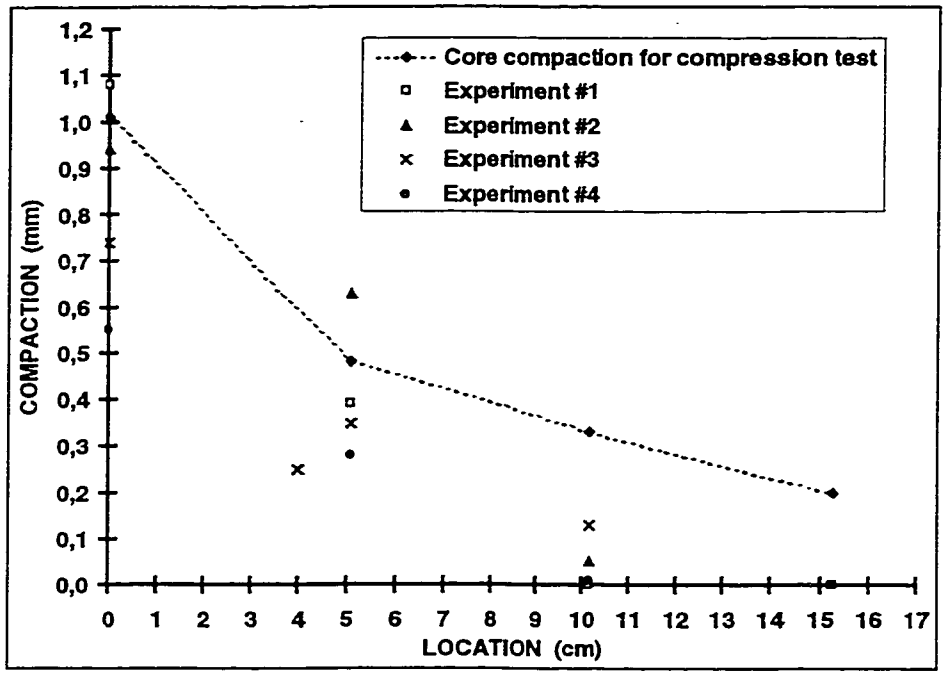

Figure 2.13 Foam core compaction during filling at various locations in the cavity for a core density of 0.09 gr./cc

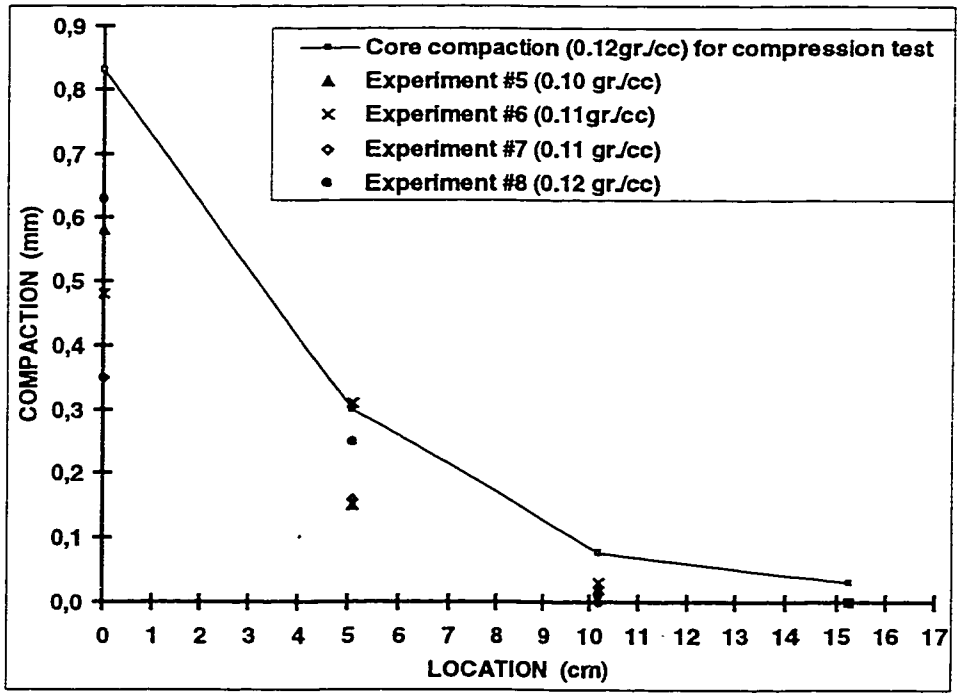

Figure 2.14 Foam core compaction during filling at various locations in the cavity for various foam densities

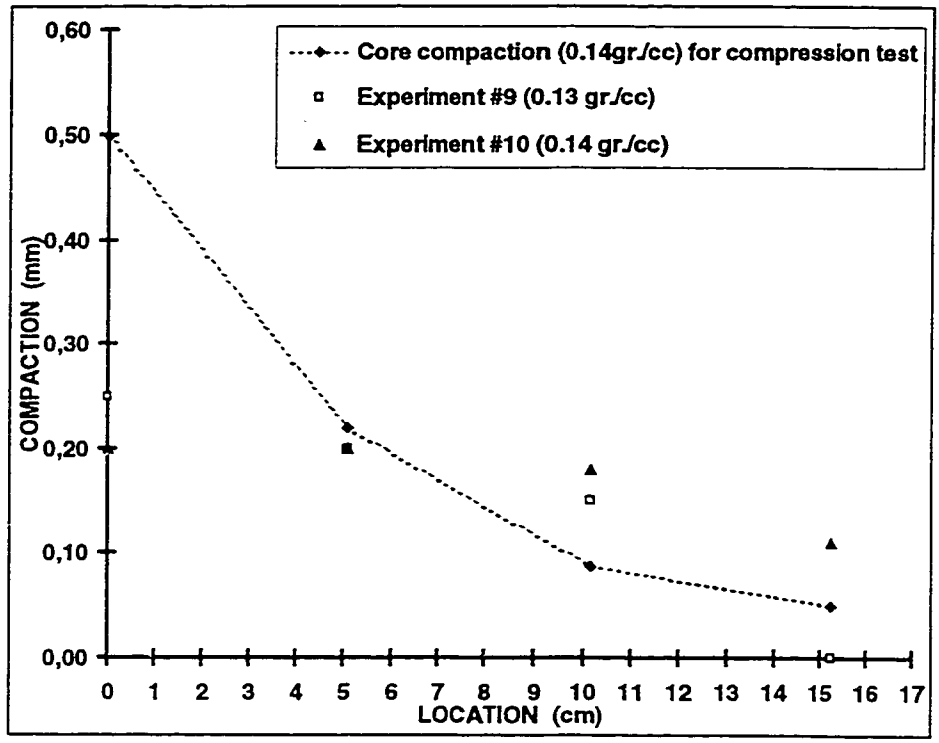

Figure 2.15 Foam core compaction during filling at various locations in the cavity for various foam densities

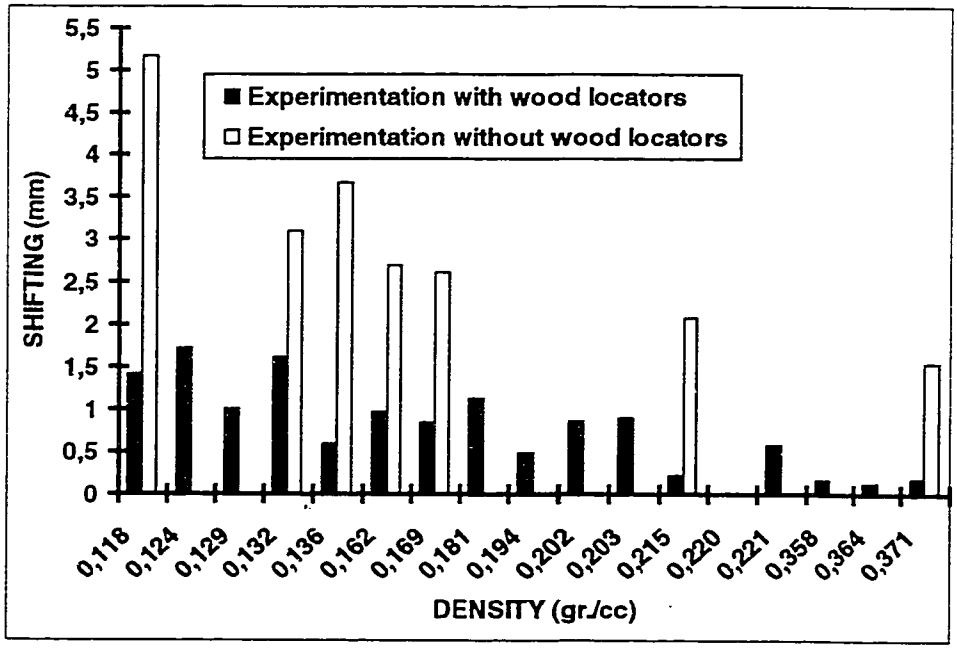

Figure 2.16 Small core shifting in the "X" direction for various foam densities

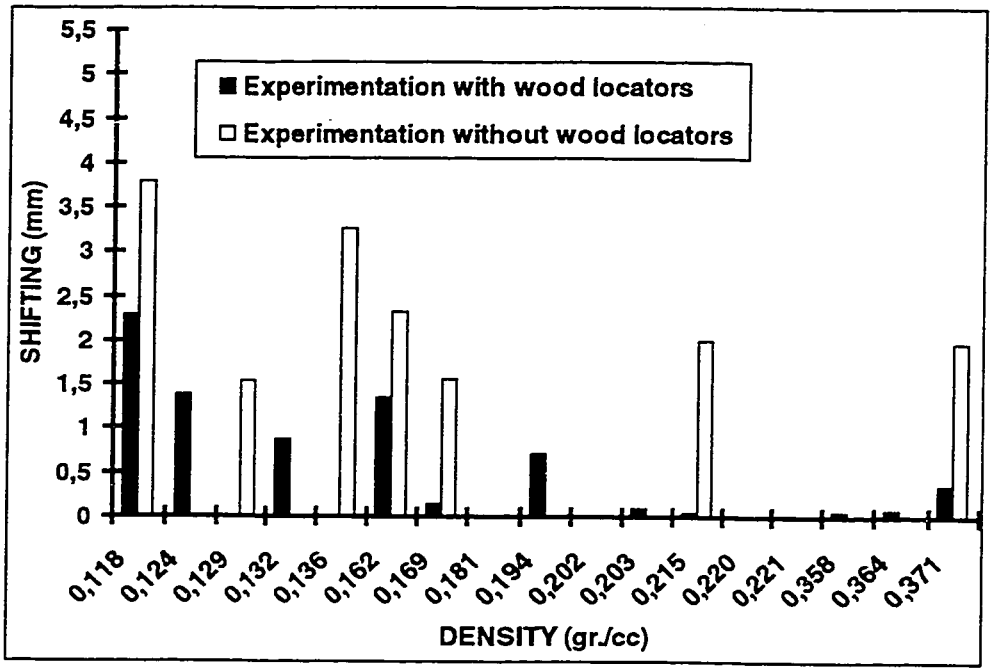

Figure 2.17 Small core shifting in the "Y" direction for various foam densities

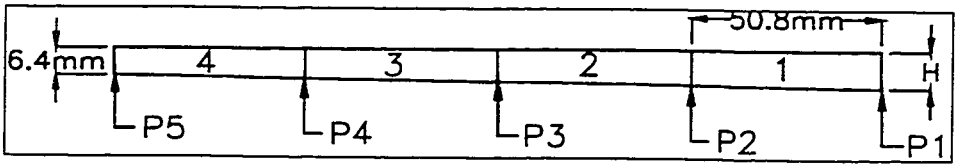

Figure 2.18 Variation of the skin thickness for flow simulation with RTMFLOT

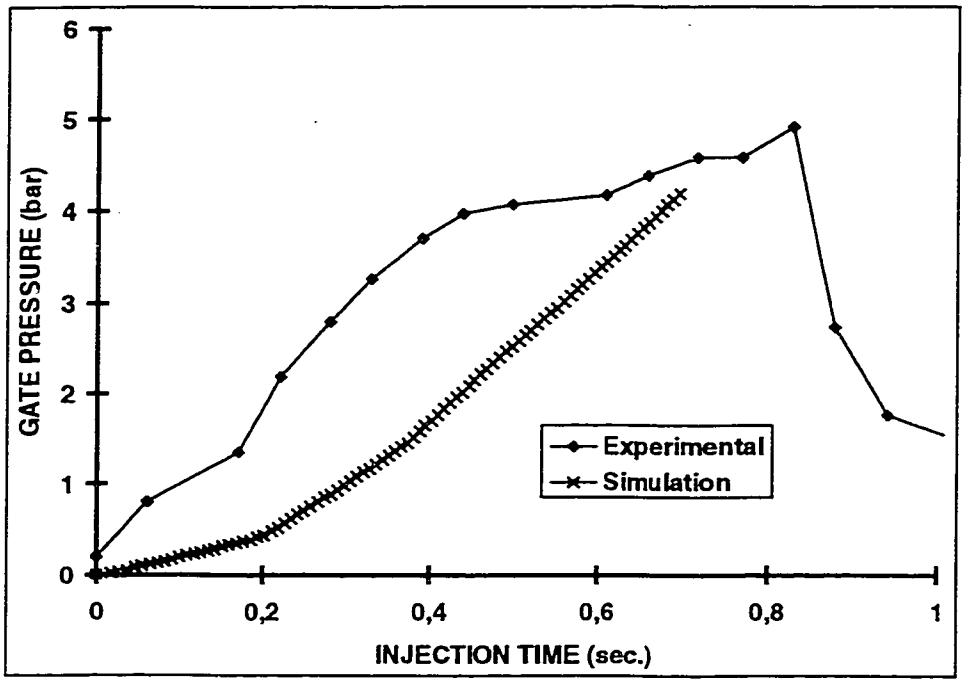

Figure 2.19 Experimental and simulated gate pressure for a plaque molded with foam core of 0.09gr./cc

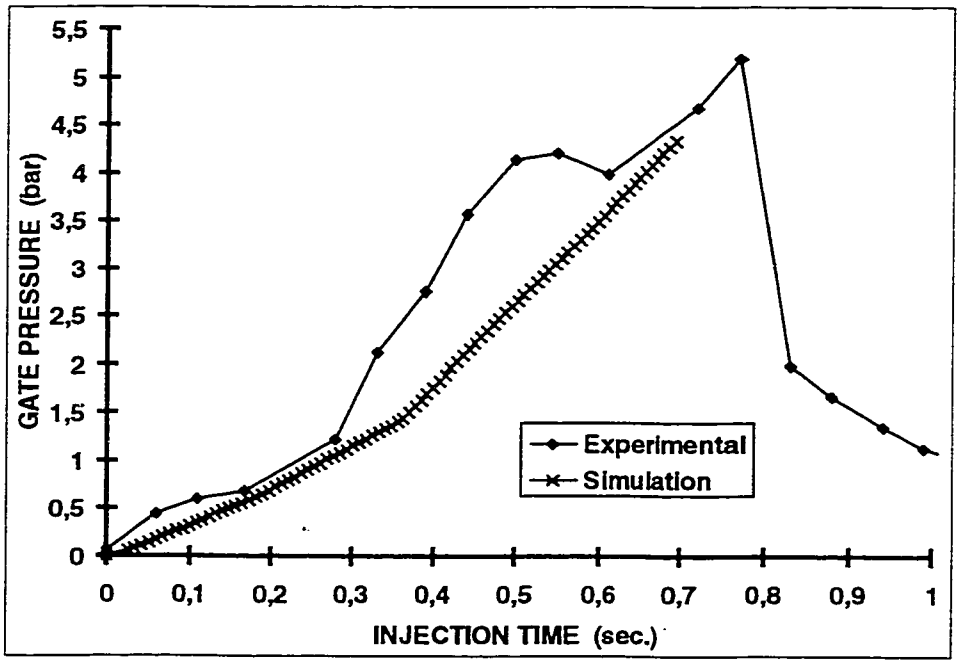

Figure 2.20 Experimental and simulated gate pressure for a plaque molded with foam core of 0.11gr./cc

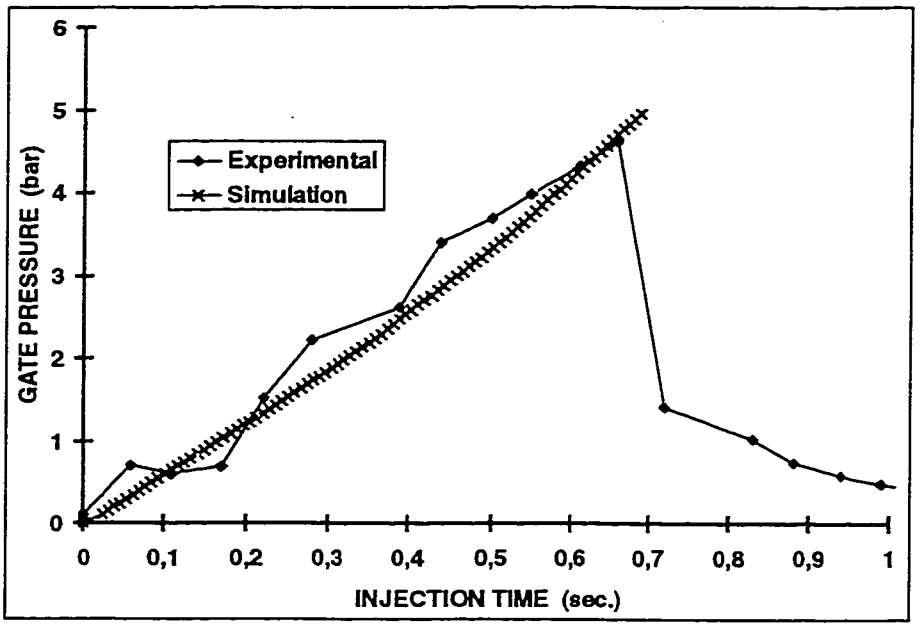

Figure 2.21 Experimental and simulated gate pressure for a plaque molded with foam core of 0.13gr./cc

2.11 TABLES

Table 2.1 Compression modulus @ 80°C for polyurethane foam

Foam density (gr/cm^3)	Comp. modulus E_1 (mPa)	Comp. modulus E_2 (mPa)	Max. Pressure (bar)
0.09	2.3	12.3	5.1
0.10	5.0	12.9	7.3
0.12	9.4	14.4	7.5
0.14	14.3	26.2	10.4
0.18	12.6	26.2	13.6
0.21	10.1	21.0	15.2
0.26	15.5	52.0	26.8
0.35	12.0	50.0	43.0

Table 2.2 Resin properties and supplier

Resin Type & supplier	Viscosity (mPa-s)	Density ($gr./cm^3$)	Gel Time	Injection System
Vinyl Ester Ashland Q6055	255 @ 25°C	1.1	45s @ 60°C	RTM
Polyurethane ICI RIMline GMR-5000 2.4:1 (ISO:POLY)	200 @ 25°C 20 @ 80°C	1.185	5s @ 80°C	SRIM

Table 2.3 Reinforcement data

Fabric name	Fabric description	Nb of layers	Surface density per layer ($gr./cm^2$)	Nominal preform thickness (mm)	Nominal fiber Vf (%)	Global permeability K (m^2)
UNIFILO U750-450	Continuous random glass fiber	6	0.0618	6.35	22	2.1 E -9
BRAIDED GLASS	Glass fiber ±45°/0°	3	0.1338	4.5	35	N/A

Table 2.4 Polyurethane foam plaque compaction results during mold filling for various core densities for the following molding conditions : 6 Unifilo U750 layers, Vf = 22%, Nominal foam thickness = 19.0 mm, Q = 400 gr/sec, Inj. time = 0.7 sec

Exp.	Density	Foam core compactions				Maximum in mold pressure			
	(gr./cc)	Loc. 1 (mm)	Loc. 2 (mm)	Loc. 3 (mm)	Loc. 4 (mm)	P1 (bar)	P2 (bar)	P3 (bar)	P4 (bar)
1	0.085	1.08	0.39	0.00	0.00	4.92	2.10	0.69	0.35
2	0.085	0.94	0.63	0.05	0.00	5.16	1.89	0.93	0.00
3	0.087	0.74	0.35	0.13	N/A	4.44	1.62	0.79	0.00
4	0.090	0.55	0.28	0.00	0.00	4.20	1.75	0.71	0.00
Av.	**0.087**	**0.83**	**.41**	**0.05**	**0.00**	**4.68**	**1.84**	**0.78**	**0.09**
5	0.100	0.58	0.15	0.00	0.00	5.56	1.67	0.35	0.07
6	0.113	0.48	0.31	0.00	0.00	6.00	2.00	0.34	0.10
7	0.114	0.35	0.16	0.00	0.00	5.18	1.72	1.20	0.99
8	0.117	0.63	0.25	0.00	0.00	6.10	1.68	0.32	0.22
Av.	**0.111**	**0.51**	**0.22**	**0.00**	**0.00**	**5.71**	**1.77**	**0.55**	**0.35**
9	0.130	0.25	0.20	0.15	0.00	4.62	0.84	0.00	0.00
10	0.135	0.20	0.20	0.18	0.11	6.70	2.29	0.88	0.30
Av.	**0.133**	**0.23**	**0.20**	**0.17**	**0.06**	**5.66**	**1.57**	**0.44**	**0.15**

Table 2.5 Polyurethane Small Core average shifting and compaction without locator (3 braid layers, Vf=35%, Q=150gr/sec, inj. Time=2.5 sec)

Exp.	Foam density (gr./cc)	Max.in mold pressure X and Y Directions (bar)	Foam core shifting		Foam core compaction		Min. laminate thickness X and Y Directions (mm)	Braid thick. from comp. test at max. in-mold pressure (mm)
			X Direction (mm)	Y Direction (mm)	X Direction (mm/mm)	Y Direction (mm/mm)		
1	0.120	10.2	2.49	3.00	0.038	0.031	3.12	2.36
2	0.131	5.0	2.85	1.42	0.003	0.005	3.00	2.49
3	0.136	8.8	2.62	2.99	0.015	0.010	2.91	2.39
4	0.165	13.4	2.66	2.32	0.000	0.000	3.05	2.31
5	0.172	10.5	2.59	1.56	0.000	0.000	3.04	2.36
6	0.212	11.6	1.75	1.99	0.004	0.000	3.37	2.34
7	0.386	30.6	1.52	1.96	0.000	0.000	3.44	2.14

Table 2.6 Polyurethane Small Core average shifting and compaction with 2mm thick wood locators (3 braid layers, Vf=35%, Q=150gr/sec, Inj. Time = 2.5 sec)

Exp.	Density (gr/cc)	Max.in mold pressure X and Y Directions (bar)	Foam core shifting		Min. laminate thickness X and Y Directions (mm)
			X Direction (mm)	Y Direction (mm)	
8	0.118	6.2	0.65	1.38	3.88
9	0.124	8.7	0.68	0.79	4.07
10	0.129	6.5	0.49	0.00	4.25
11	0.132	9.8	0.48	0.28	4.12
12	0.162	12.7	0.34	1.34	3.86
13	0.169	11.6	0.83	0.14	4.15
14	0.181	14.5	0.24	1.87	3.56
15	0.194	11.5	0.20	0.71	4.03
16	0.202	14.4	0.85	1.33	3.87
17	0.203	9.7	0.84	0.09	4.05
18	0.215	17.3	0.07	0.04	4.28
19	0.220	17.5	0.08	1.25	3.92
20	0.221	13.4	0.21	0.02	4.37
21	0.358	27.0	0.15	0.05	4.34
22	0.364	33.0	0.00	0.06	4.42
23	0.371	14.2	0.00	0.27	4.44

Table 2.7 Resin and part weights for Polyurethane Small Core with wood locators

Experiment	Density (gr/cc)	Part weigth (g)	Resin weigth (g)	Resin % in part (%)
8	0.118	775	307	40
9	0.124	800	345	43
10	0.129	781	314	40
11	0.132	825	357	43
12	0.162	795	308	39
13	0.169	819	315	38
14	0.181	803	306	38
15	0.194	814	291	36
16	0.202	825	306	37
17	0.203	802	274	34
18	0.215	842	314	37
19	0.220	853	329	39
20	0.221	827	295	36
21	0.358	909	278	31
22	0.364	889	256	29
23	0.371	908	257	28

Table 2.8 Permeability and laminate thickness for the equivalent stepwise skin for three foam densities

Simulation	Density (gr./cc)	Zone	Porosity	K global (1E-9 m²)	Lam. Thickness (mm)
S1	0.09	1	0.85	6.29	7.0
		2	0.80	2.80	6.6
		3	0.78	2.14	6.4
		4	0.78	2.14	6.4
S2	0.12	1	0.83	4.42	6.8
		2	0.82	3.77	6.7
		3	0.78	2.14	6.4
		4	0.78	2.14	6.4
S3	0.14	1	0.80	2.80	6.6
		2	0.80	2.80	6.6
		3	0.79	2.43	6.5
		4	0.78	2.14	6.4

PRÉSENTATION DU CHAPITRE 3

Le chapitre 3 est consacré à l'étude du procédé CRTM (Compression Resin Transfer Molding) et de ses variantes possibles. Le CRTM a pour but d'obtenir une pièce composite possédant une plus grande concentration de fibre que la traditionnelle injection RTM (Resin Transfer Molding). Le procédé consiste à placer une préforme de fibre de verre dans les cavités d'un moule tout en les gardant partiellement ouvertes. Après l'injection, le moule est fermé forçant ainsi la résine à complètement mouiller les fibres.

Deux types d'expérimentations ont été pratiquées. La première consiste à utiliser une préforme de tissu de verre thermoformée à l'épaisseur finale constante de la pièce. Celle-ci est alors déposée dans un moule plaque rectangulaire légèrement ouvert, laissant un canal vide entre la paroi supérieure du moule et la surface de la préforme. La résine est injectée dans la cavité vide et par la suite le moule est fermé, permettant un mouillage uniforme de la préforme.

La seconde expérimentation utilise des mats de fibres de verre aléatoires continus remplissant complètement une cavité de moule légèrement entrouverte. Lors de l'injection, la résine va graduellement mouiller le renfort à travers son épaisseur. La nouvelle approche expérimentée est d'injecter la résine en même

temps que le moule est fermé. Cette méthode s'apparente à la déformation des coeurs de mousse et à la compaction des renforts discuté au Chapitre 2 du présent ouvrage. Dans les deux cas, nous sommes en présence d'une loi de Darcy non-linéaire, c'est à dire ou la perméabilité du renfort varie en fonction du temps.

CHAPITRE 3

EXPERIMENTAL ANALYSIS OF MOLD FILLING IN COMPRESSION RESIN TRANSFER MOLDING

S. Wirth, École Polytechnique de Montréal, Qué., Canada
R. Gauvin, École Polytechnique de Montréal, Qué., Canada

3.1 ABSTRACT

Over the years, several modifications of the more standard liquid molding processes such as SRIM and RTM have been proposed. Among them the Compression Resin Transfer Molding (CRTM) presents a great interest. In that process, like in RTM, the fiber preform is preplaced in a mold and then, a liquid resin is injected. In CRTM however, the mold is kept slightly open during the resin injection. Once the necessary amount of resin is injected, the final closing is done and the resin filled the entire cavity. The main advantage of this technique is to reduce the necessary injection pressure and to ease the molding of parts with high fiber.

In this paper, results are reported for two series of plaque molding experiments. In all cases filling time and pressure distribution in the cavity was recorded. In the first series, vinyl ester resin was injected in a slightly open cavity where a thermoformed glass fiber preform had been placed. In this case an open gap was present on the top of the preform which eased considerably the filling. The mold was then closed to final part thickness. In this case, the resin injection time

was extremely short and most of filling and wetting time was elevated to the final closing of the cavity.

In the second set of experiments, continuous stand glass fiber mat was used. Because of their nature, the layers of glass mat completely filled in partially closed cavity. As oppose to the previous experiments, in this case, the cavity was closed during the resin injection. The closing time was chosen in such a way that filling and closing occur simultaneously. Since the reinforcement permeability is reduced during injection, the filling rate was much slower at the end. The data gathered with these experiments could also be used to validate the modeling of foam core parts molding when resin pressure crushes the core.

3.2 INTRODUCTION

One of the goals of the composite industry using Liquid Composite Molding (LCM) processes is to manufacture composite parts with better mechanical properties, increased fiber volume fraction and reduced cycle time. Over the years, several modifications of the Resin Transfer Molding (RTM) process have been proposed to improve the cycle time or to increase the fiber volume fraction and by doing so, the mechanical properties of the finished product. Among them, the moving wall process of the more commonly called Compression Resin Transfer Molding (CRTM). In that process, the fiber preform is placed into the cavity and the resin is injected while to mold is kept partially

open. Once the required amount of resin has been injected, the mold is closed, forcing the liquid resin to fill out the entire cavity like in compression molding. This modification eases the molding of parts with a high fiber content, using low-pressure pump, since the press will provide the necessary pressure to completely wet out the fiber preform.

In this paper, two limit cases are studied. In the first one, a thermoformable fabric is used. After the reinforcement has been thermoformed, it is compacted and the preform has almost its final thickness.

When placed in a slightly open mold, it leaves an open gap between the preform and the mold wall, allowing the resin to rapidly fill that gap before it penetrates through the thickness when the mold is finally closed. In practice, this is the most interesting case for CRTM because many higher fiber fractions can be achieve, even with low pressure pumping unit. This is the first case being investigated here. The second one is when a fairly loose reinforcement such a continuous strand mats is use. Then even if the mold is not completely closed, the reinforcement fits the entire height of the slightly open cavity and during injection the resin impregnate the loosen reinforcement through the thickness up to a fraction of the entire cavity surface. The final closing forces the resin to fill the remaining of the cavity. In practice, this case is of limited interest because conventional RTM with continuous strand mat is easily done. In this paper, we

added a modification to this case. In our experiments, the mold is closed during the resin injection. The closing speed is chosen in such a way that injection and closing take roughly the same time. A part from their interest as a CRTM process, the results obtained from these experiments will be extremely useful to validate a Darcy's law model based on a permeability variation in function of time. Such a non linear permeability occurs during RTM manufacturing of foamed core parts. Depending on the foam properties and the injection pressure in most cases, core crushing occurs during molding resulting in a non-linear Darcy's flow.

3.3 MATERIAL AND EQUIPMENT

3.3.1 Molding Facilities

Figure 3.1 shows a top view of the picture frame cavity used in the investigation for the two sets of experiments. The picture frame is made out of rubber strip to accommodate thickness variations. As illustrated in Figure 3.2, all plaques were molded with the reinforcement placed on the bottom plate, where the pressure transducers and the thermocouples are mounted. Six pressure transducers (P_1 to P_6) and nine thermocouples (T_1 to T_9) are located in the bottom mold plate. Thermocouples were used to determine the resin flow front progression during the part filling. Since the mold and the reinforcement were heated at 60°C and the resin was injected at room temperature, it was easy to

read the flow front progression in the fabric with the thermocouples. For each experiment, the quantity of resin needed to fill the part was carefully monitored.

For the first series of experiments, the mold is open to create an open cavity of thickness H. The resin was then injected with a pressure pot in the empty cavity to fill the gap on top of the preform, as illustrated in Figure 3.2. Right after the injection, the mold was closed to complete the wet out of the fabric. The initial total cavity height (H) used for the experiments were between 5 to 9mm. For each of these experiments, a 3.1mm thick fiberglass preform, 75cm in length was used, giving a final fiber volume fraction $V_f = 41\%$ in the part. In all cases, a slow clamping speed of approximately 0.13mm/sec was kept for all the experiments. For the second series of experiments, the mold was opened to create a cavity thickness of 5.1mm. But in that case, the cavity opening was filled up with 3 layers of continuous strand glass fiber mats, 60cm in length, giving an initial Vf of 11%. As describe in Figure 3.3, the mold cavity was gradually closed with a constant speed of 0.09 mm/sec during the resin injection until it reaches the final part thickness of 3.1mm which corresponds to a fiber volume fraction $V_f = 18\%$). Since filling and closing occurred simultaneously, the part filling time and the mold closing time were carefully matched for these experiments.

3.3.2 Resin and reinforcements

A polyester resin having a viscosity of 0.160 Pa-s, a density of 1.1 and a gel time of 20 minutes at 25°C were used for all experiments. For the first series of experiments, a Brochier thermoformable fabric EXB-315-E02-120 was selected because of its ability to be preformed. This fabric is manufactured with an epoxy powder sprinkled on the glass fibers for thermoforming. A rigid board like preform of 3.1mm thick was obtained with 10 layers of reinforcement compressed in a heated cavity. For the second series of experiments, three layers of OCF-8610 continuous strand mat from ovens corning were use. The reinforcement properties are listed in Table 3.1. The permeability of the preformed fabrics and the mats were measured in the warp and weft directions in a unidirectional flow set up device available in our laboratory. The permeability Kz in the thickness direction was also measured in our lab.

3.4 EXPERIMENTAL

The polyester resin was injected at a constant flow pressure of 69 Kpa with the Brochier preform and 200 Kpa with the OCF. A PC linked to the molding equipment allowed the display of the temperature, the pressure and the upper plateau displacement during the experiments. The resin progression in the mold was measured both with the thermocouples and the pressure transducers. For the thermocouples, a sudden decrease of their temperature indicated a contact with the resin.

Table 3.2 shows the data collected for all of the tests with the Brochier preform. Under the "Cycle Time" title, the resin injection time column show typical values around 2 seconds. These very low injection times were obtained because the resin is injected in the open gap. The next column, the wait time, is the time elapsed between the end of the injection and the beginning of the final clamping activation. The cycle time is the summation of the injection time, the wait time and the clamping. The next series of information concern the flow front progression. The first column gives the resin front position in the gap after injection and before clamping time. The next one give the average resin flow front speed in the saturated reinforcement as measured with the thermocouple position in the bottom plate. Finally the mold constant closing speed is given. The final set of results gives the recorded pressure during some experiments, for the six pressure transducers located in the bottom plaque cavity. Referring to Figure 3.2, one can see that the resin progressively penetrates from left to right and from top to bottom, the saturated length is then measured with the thermocouples on the bottom plate.

Table 3.3 shows the data collected for all of the second series of experiments with the OCF continuous strand mat. The two columns under the heading cycle time show that the clamping time was slightly longer than the injection time. The average injection time was 19 seconds and the average clamping time 24 seconds. So, after the resin injection was completed, the mold

still compressed the laminate to remove the excess of resin. An average flow front speed was calculated for each experiment, although it is not necessarily constant. The global flow front average speed during the experiments was 3.1 cm/sec. The final set of results gives the pressure for the six transducers located in the bottom plaque. The pressure values reported in Table 3.3 were measured just at the end of the resin injection. The saturated length of the mat was measured with the thermocouples located on the bottom plate.

3.5 RESULTS AND DISCUSSION

The curves in Figure 3.4 represent the reinforcement saturated length during the resin injection time and the mold clamping time for five experiments. Each one used the 3.1mm thick glass fiber preform made from the Brochier EB-315 fabric described earlier in mold cavity openings varying from 5 to 9mm. The circled values on the curves indicate the beginning of the mold clamping after the resin injection. The first half of the curve, before the mold clamping, shows a fabric wet out length more important for smaller cavity openings which is normal. The last portion of the curves gives the progression of the reinforcement-saturated length under the influence of the mold clamping. In that case, the resin flow is directly related to the mold clamping speed. Figure 3.5 shows the cavity height as a function of the saturated length. It shows that for the largest opening, the resin barely reaches the bottom of the cavity during the injection, before the final clamping begins. The mold closing speed given in Table 3.2 was calculated

from the curves of Figure 3.6. The declining slopes of the curves in Figure 3.6 are similar, indicating a similar closing speed. The average closing speed for all the experiment is 0.13mm/sec.

Figure 3.7 gives the pressure distribution near the line gate (P1) for different initial cavity heights. As shown, once the injection is completed, the resin has not yet reached the cavity bottom. So begins about 6 to 9 seconds after the start, the cavity has to be closed considerably before any pressure can be felt on the bottom of the cavity near the gate, especially for large initial heights. Since the planar permeability of the preform is much lower then the transverse permeability for a larger initial gap, during injection, the resin stays closer to the gates. Then, during closing, a larger portion of the preform must be saturated through a planar flow in the reinforcement instead of a through the thickness flow. This explains why the maximum recorded pressure reaches higher values for larger initial gaps.

A typical cavity pressure distribution from the 6 pressure transducer locations is presented in Figure 3.8 for a 7mm initial cavity height. Initially, since the resin has not reached the bottom, there is no reading. After that, the resin pressure builds up from left to right in the cavity. Then at the end of clamping (EC), after 30 seconds, the pressure at center is higher than on both ends. To better illustrate that, Figure 3.9 shows the pressure distribution in the cavity at

time steps shown by the vertical dotted lines in Figure 3.8. The preform-saturated length is shown for 20 and 24 seconds on the cavity drawing appearing at the top of Figure 3.9. During the mold clamping, at 20, 24 and 27 seconds, the preform is saturated with a linear pressure distribution from left to right. Near the end of closing and right after it, the pressure is higher at center. But the more important phenomenon is the tremendous rise of pressure near the end of the cycle.

Finally, the second set of results was obtained with a glass fiber mat and for injection and mold closing occurring simultaneously. The curves in Figure 3.10 represent the reinforcement-saturated length during the resin injection time and the mold clamping time for the experiments 2, 5, 6 and 7 of Table 3.3.

Since the permeability varies slightly during closing, going from 9.9E-9m^2 for V_f=11% to 4.9E-9m^2 for V_f =18%, the saturated length versus pressure given in Figure 3.10 is not perfectly linear, even if the injection pressure is kept constant at 200 KPa. Figure 3.11 shows the cavity height versus the saturated length. There again a slight deviation from a straight live is observed.

To illustrate what is going on in the cavity during such an experiment, Figure 3.12, 3.13 and 3.14 given the results for the experiment number 6 of Table 3.3. Figure 3.12 and 3.13 present the resin pressure at various locations

on the cavity bottom as a function of time and the reinforcement saturated length respectively. As one can see, the pressure varies considerably throughout the cavity. As seen on both graphs, maximum values occur at the end of injection which what one would expect. In Figure 3.13, a pressure reading can be observes for the transducers P4, P5 and P6. Because the mold was clamped during the injection, it seems that the dry OCF reinforcement pushed on the pressure transducers before the resin reaches them.

Figure 3.14 shows the pressure distribution along the cavity length at various time steps. The chosen time steps are indicated by the vertical dotted lines appearing in Figure 3.12. During the whole experiment, resin pressure decreases from the injection part towards the resin front. At the end of injection (E.I.) however, it has a convex shape and at center, surpass the injection pressure of 200 KPa. It then diminishes throughout the cavity because the excess of resin was allowed to leak at the right end of the cavity.

3.6 CONCLUSION

It was shown that Compression Resin Transfer Molding (CRTM) is feasible and can permit the molding of parts with a high fiber volume fraction, even with a pumping unit of low capacity. Especially with thermoformable fabrics, the compact preform leaves an open gap in the partially closed cavity, which is extremely easy to fill. The molder can then rely on its press to generate

the necessary pressure to impregnate the entire preform. One should be careful however, for uneven thickness since large pressure difference may be generated in the cavity. These differences however, are much less important than one would encounter in Sheet Molding Compound Molding for instance.

Finally, CRTM with low fiber volume fractions, typical of continuous strand mats, does not present any significant advantages. However, when injection and closing occurs simultaneously like is was done here, it is an elegant way to study non linear Darcy flow in a porous media which often occurs in foamed core parts molding.

3.7 ACKNOWLEDGMENTS

The authors wish to acknowledge the Fond Canadien d'aide à la recherche (FCAR) from the Province of Quebec Government and the Natural Sciences and Engineering Research Council (NSERC) of Canada for their financial support. Also, the technical support and advises from Dr. Ken Kendall from the FORD Materials Laboratory where highly appreciated.

3.8 REFERENCES

1. **GAUVIN, R. , TROCHU, F.** (1994). « RTMFLOT, un logiciel intégré et modélisation des procédés RTM », *Composites, **5**,*16-22.

2. **KENDALL, K.N.** (1994). « Component and Process Design for Liquid Composite Moulding », *Int. Conf. on design and manufacturing using Composites, ATNAM '94, Montreal.*

3. **FERLAND, P., GUITTARD, D. TROCHU, F.** (1996). « Concurrent Methods for Permeability Measurement in RTM », *Polymer Composites, **17**, 1*, 149-158.

4. **RUDD, C.D., RICE, E.V., BULMER, L.J. and LONG, A.C.** (1993). « Process Modeling and Design for Resin Transfer Molding », *Plasctic, Rubber and Composites Processing and Applications, **20**, 2,* 67-76.

5. **GAUVIN, R. and CHIBANI, M.** (1986). « The Modeling of Mold Filling in Resin Transfer Molding », *International Polymer Processing, **1** Issue 1,* 42-46.

6. **GAUVIN, R. and TROCHU, F.** (1996). « Keys Issues in Numerical Simulation of Liquid Composites Molding Processes », *Proc. of the 29th ISATA Conf., Florence,* 1107-1114.

7. **HAN, K., TREVINO, L., LEE, L. J., LIOU, M.** (1993). « Fiber Mat Deformation in Liquid Composite Molding I : Experimental Analysis », *Polymer Composites, **14**, 2,* 144-150.

8. **HAN, K., LEE, L. J., LIOU, M.** (1993). « Fiber Mat Deformation in Liquid Composite Molding II : Modeling », *Polymer Composites, **14**, 2,* 151-160.

9. **YOUND, W.B, HAN, K., FONG, L.H., LEE, L.J. and LIOU, M.J.** (1991). « Flow Simulation in Molds with Pre-placed Fiber Mats », *Polymer Composites, **12**, 6,* 391-403.

10. **GAUVIN, R., CLERK, P. LEMENN, Y., TROCHU, F.** (1994). « Compaction and Creep Behavior of Glass Reinforcement for LCM », *Proc. of the 10th Annual ASM/ESD Advanced Composites Conf., MI,* 357-367.

11. **BADDINGTON, D.A., ENOS, J.H. and COX, J.M.** (1987). « High Speed RTM of Vinyl Ester Resins », AUTOCOM-87, Dearborn, MI, EM87-351.

13. **GAUVIN, R. and CHIBANI, M.** (1988). « Modelization of the Clamping Force and Mould Filling in Resin Transfer Moulding », *43rd Annual Conference of SPI, Cincinnati Paper, # 22-C,* 1-4.

3.9 FIGURES

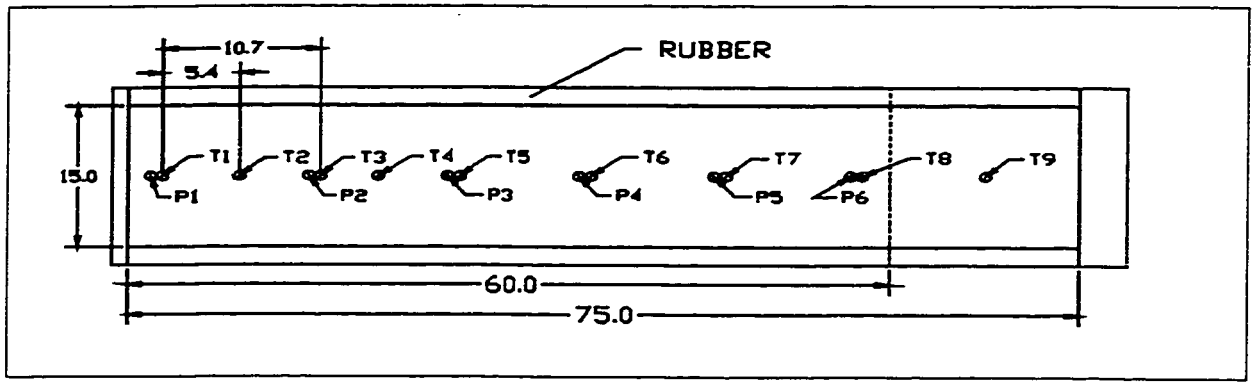

Figure 3.1 Schematic of the sensors location on the bottom plate (60cm length for OCF-8610; 75cm length for Brochier EB-315)

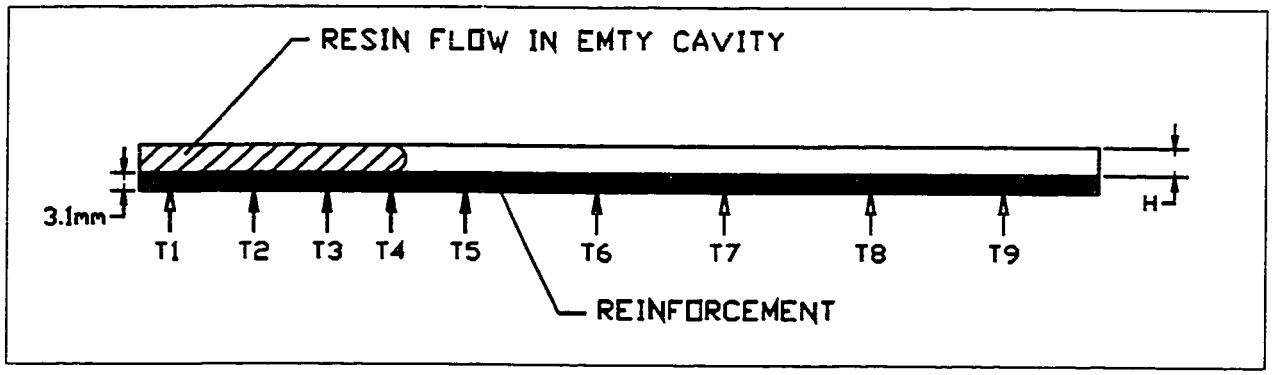

Figure 3.2 Resin flow in the partially open cavity with a Brochier preform

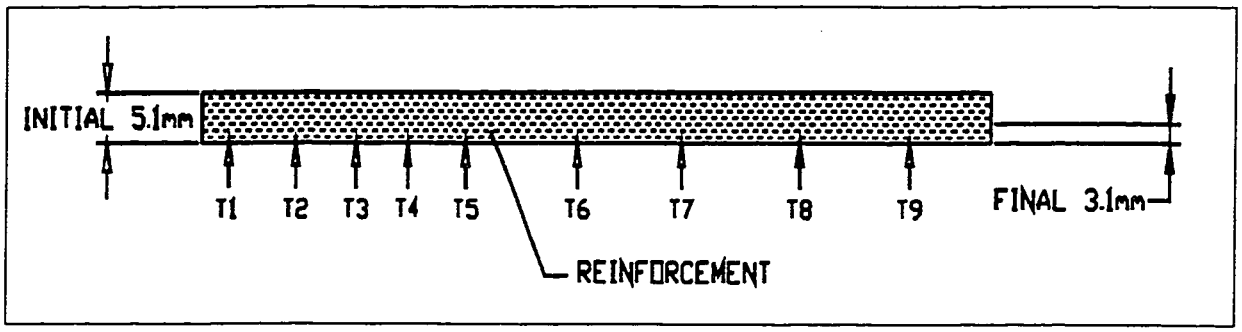

Figure 3.3 Resin flow in the partially open cavity with OCF-8610

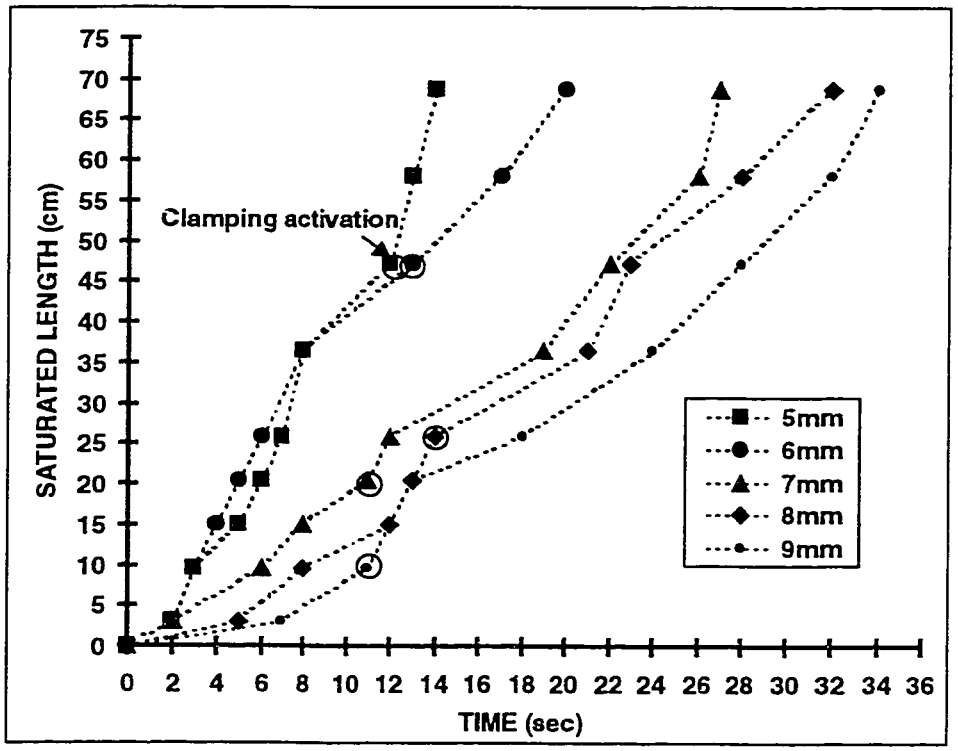

Figure 3.4 Saturated length versus time for the Brochier EB-315 preform with a V_f of 41%. Circled values identify the time when final clamping is activated after injection is stopped

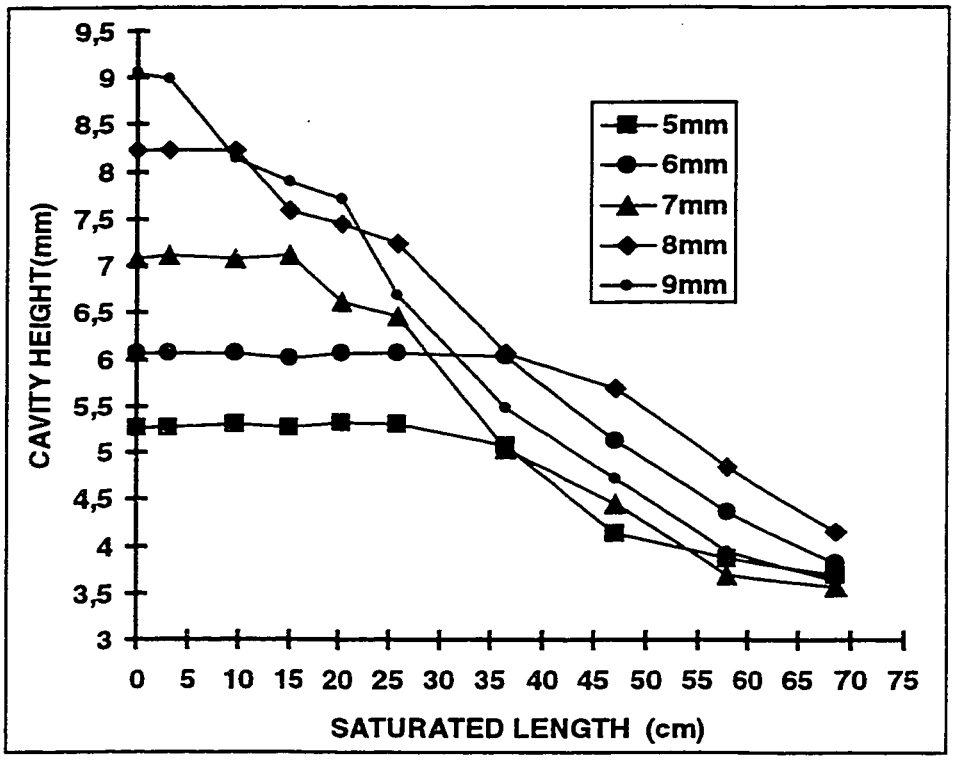

Figure 3.5 Cavity height versus saturated length for experiments with the Brochier EB-315

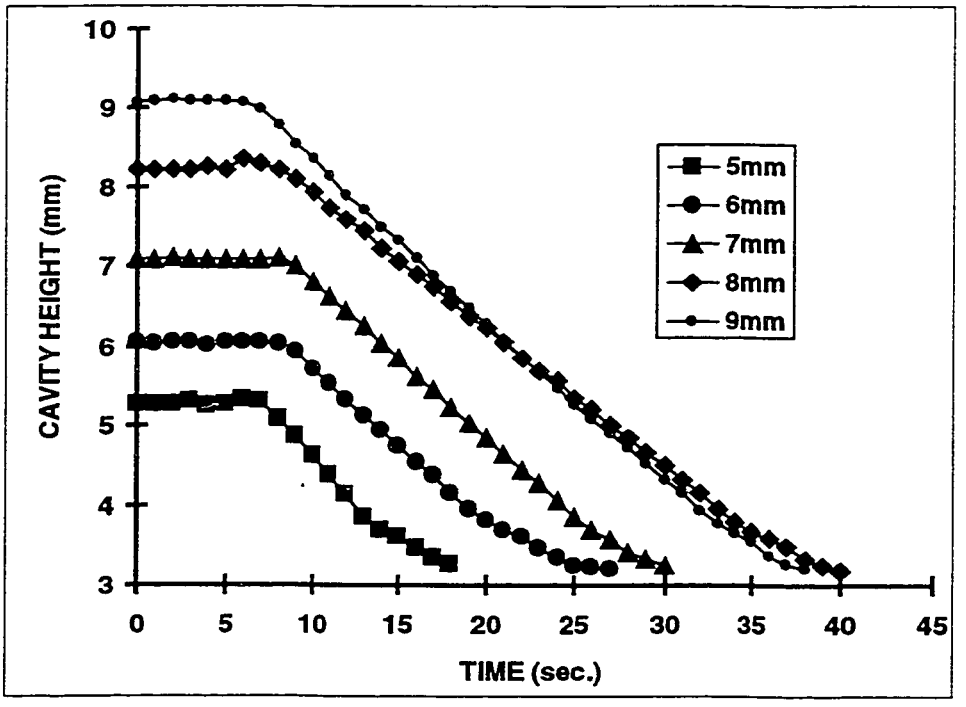

Figure 3.6 Cavity height versus time

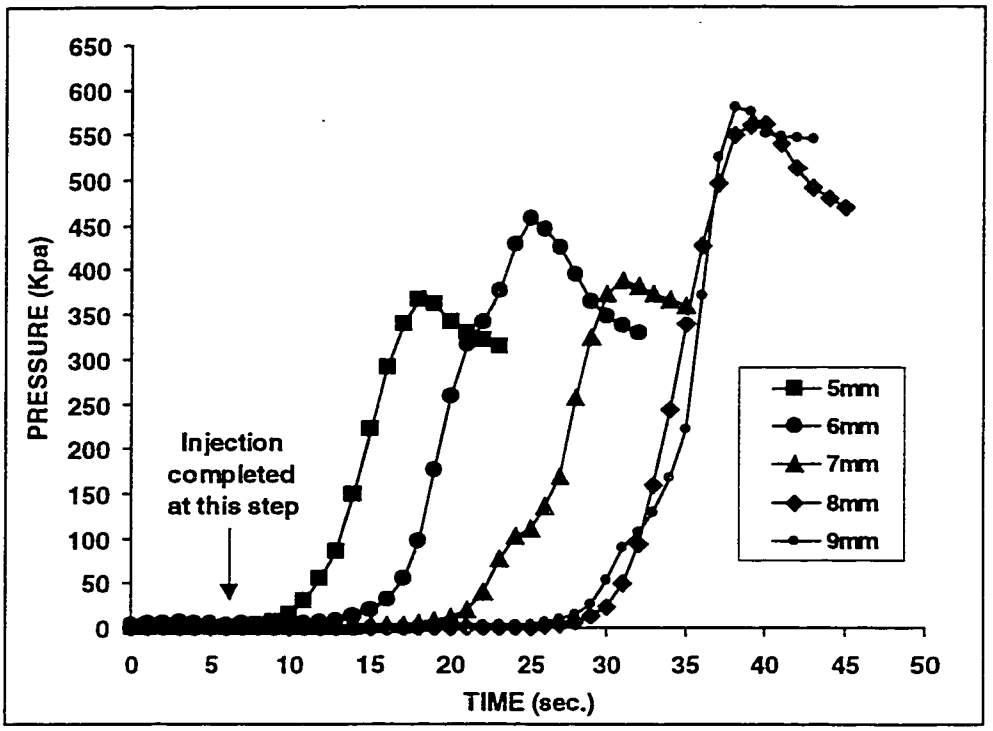

Figure 3.7 Molding pressure distribution P_1 at the line gate for experiments with a preform

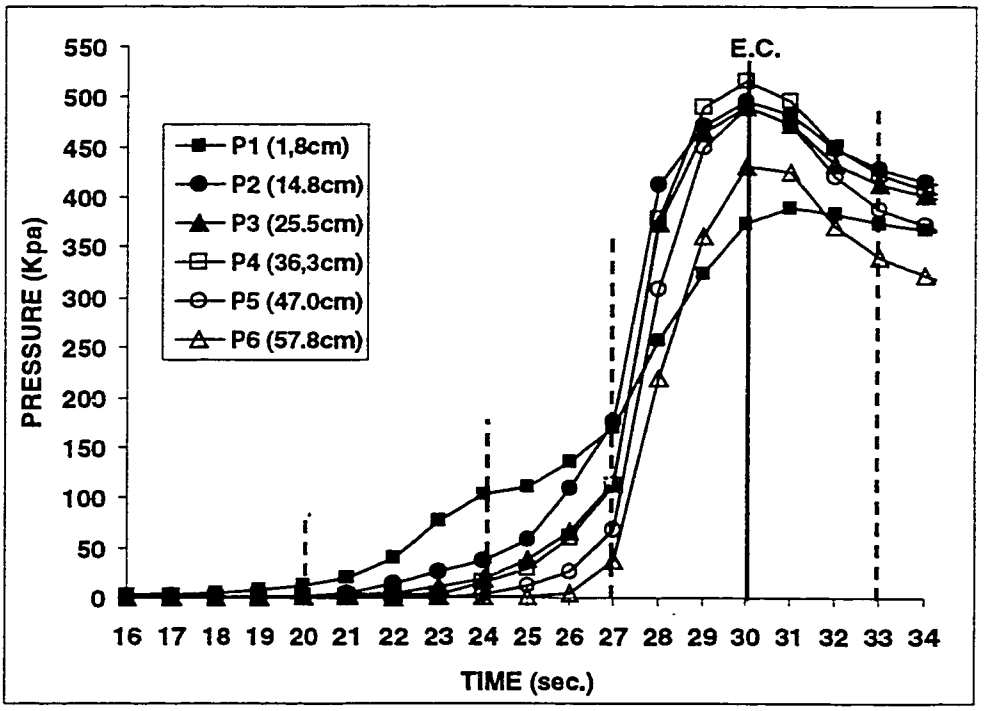

Figure 3.8 Resin pressure distribution on cavity bottom for a 7mm initial cavity height during clamping (Brochier EB-315)

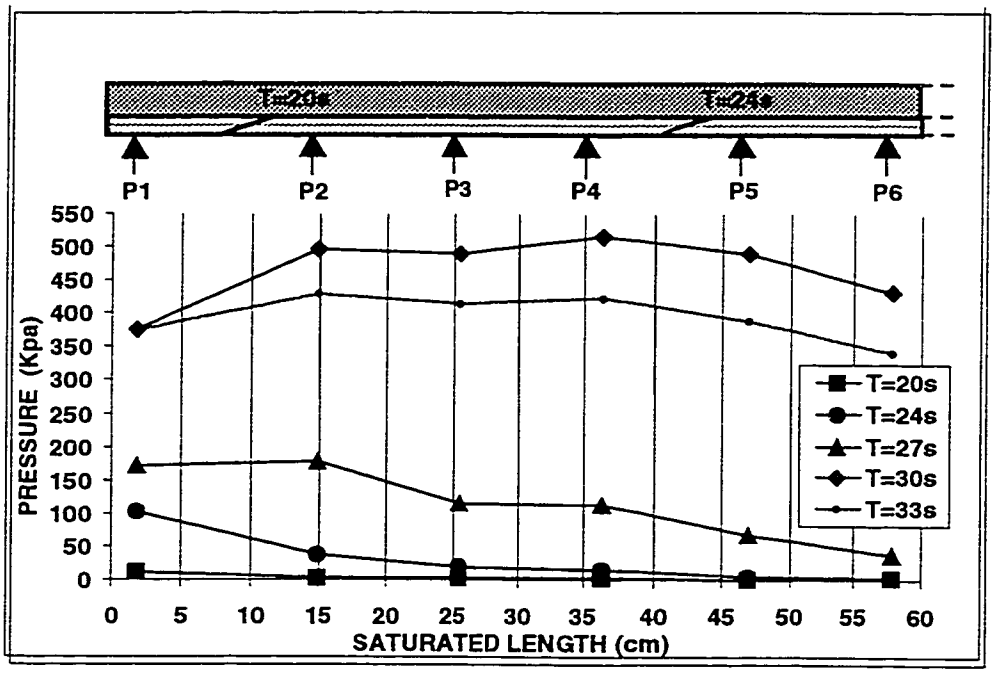

Figure 3.9 Typical pressure distribution versus saturated length during clamping (Brochier EB-315)

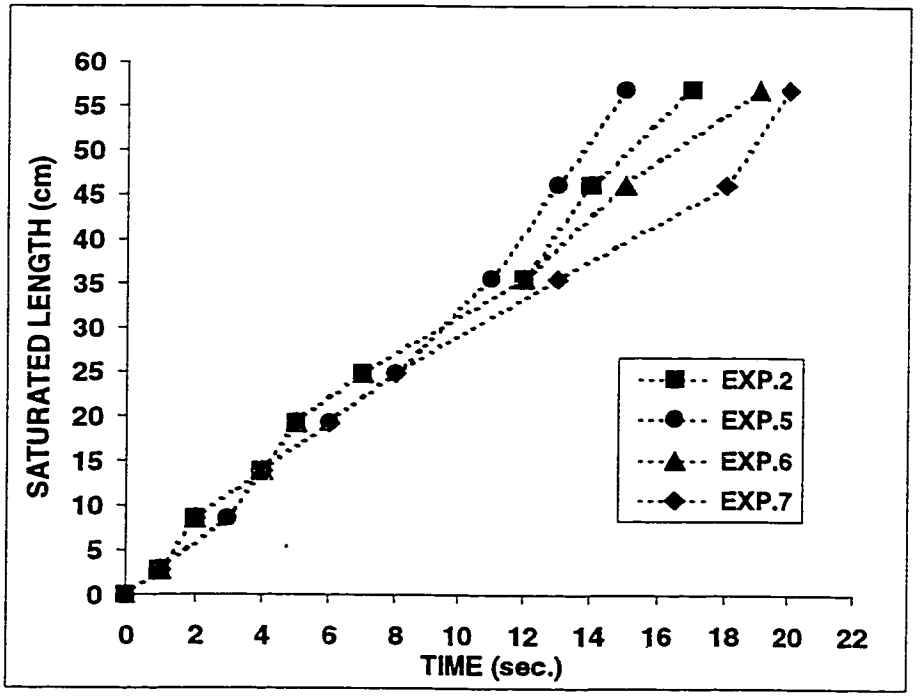

Figure 3.10 Saturated length versus time (OCF-8610)

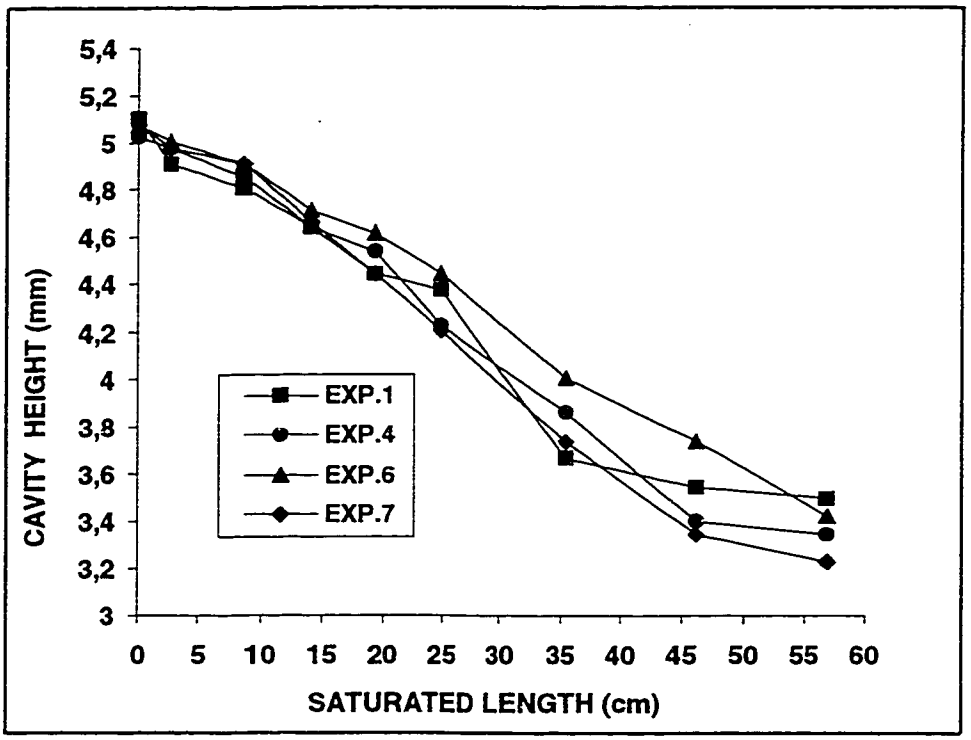

Figure 3.11 Cavity height versus the saturated length. Injection occurs during mold closing (OCF-8610).

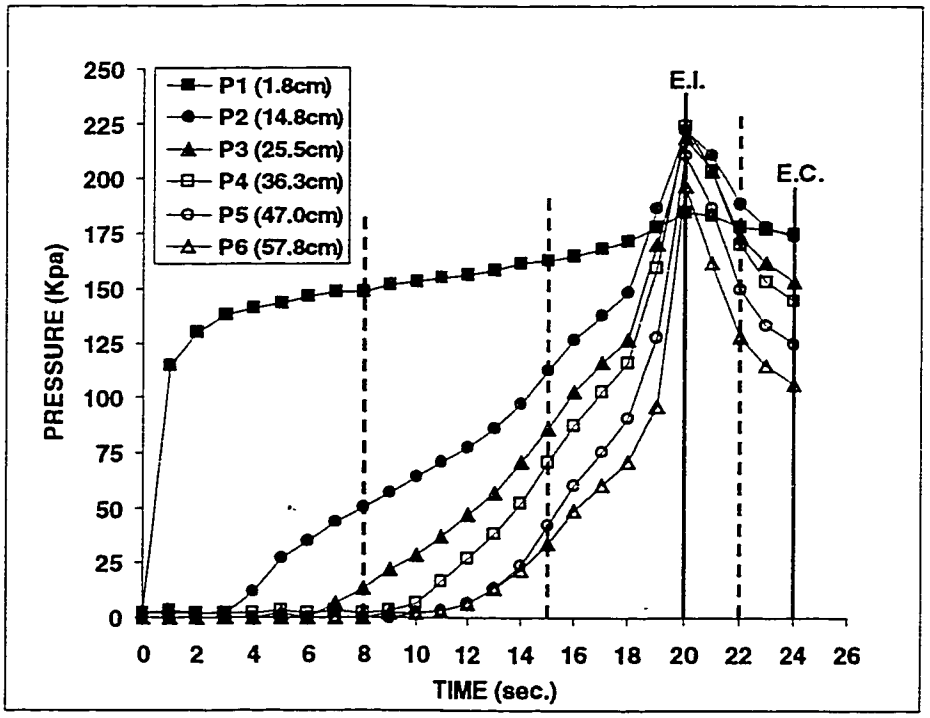

Figure 3.12 Typical pressure distribution for the Exp. 6 with OCF-8610

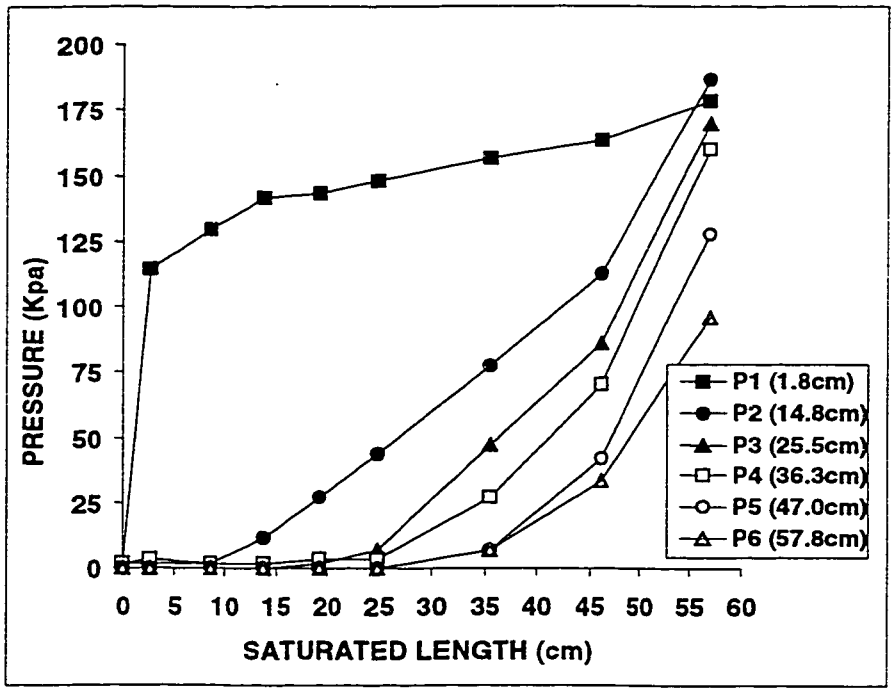

Figure 3.13 Pressure distribution versus the saturated length (Exp. 6 with OCF-8610)

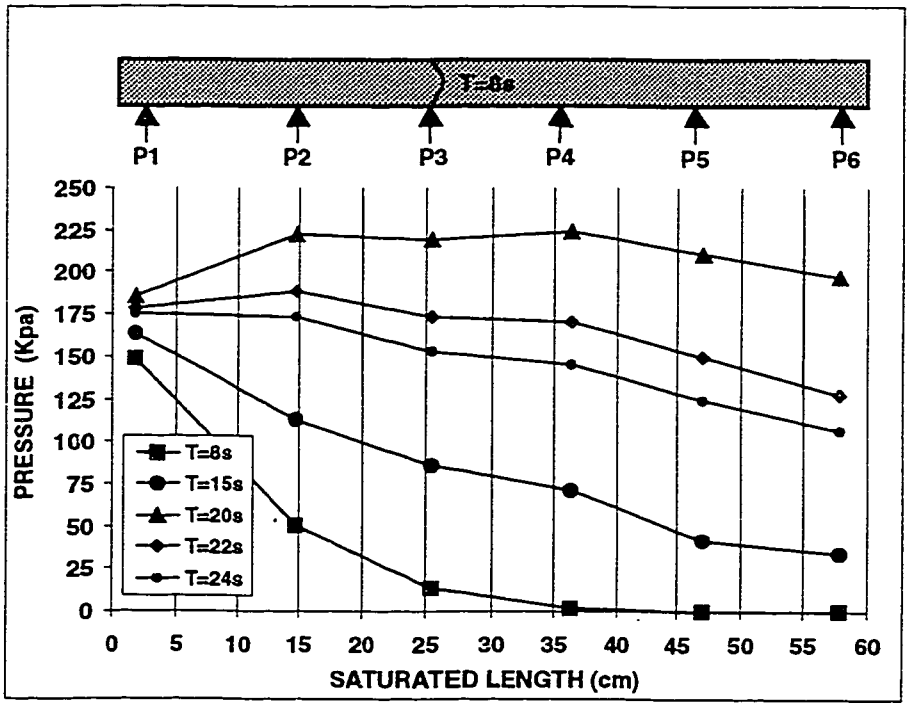

Figure 3.14 Typical pressure distribution versus the saturated length during injection and clamping for Exp. 6 with OCF-8610

3.10 TABLES

Table 3.1 Reinforcement data

Fabric Name	Fabric Description	Surface density per layer (Kg/m^2)	Nominal preform thickness (mm)	Nominal Fiber Vf (%)	Permeability Kwarp ($1E\text{-}9\ m^2$)	Permeability Kweft ($1E\text{-}9\ m^2$)	Transverse Perm. Kz ($1E\text{-}9m^2$)
BROCHIER EB-315-E02-120	Glass Fiber Fabric 0/90°	0,323	3,1	41	0,91	10,08	0,46
OCF-8610	Glass Fiber Continuous random mat	0,466	3,1	18 11	4.9 9.9	4.9 9.9	1.49 3.3

Table 3.2 Data of each experiment with Brochier EB-315 preform

	Thickness		Cycle Time				Flow Front			Maximum in mold pressure					
Exp.	Initial	Final	Inj. Time	Wait Time	Clamp Time	Cycle Time	Location in the gap before clamping	Average speed during clamping	Closing speed	P1 @ 1.8 cm	P2 @ 14.8 cm	P3 @ 25.5 cm	P4 @ 36.3 cm	P5 @ 47.0 cm	P6 @ 57.8 cm
(#)	(mm)	(mm)	(sec)	(sec)	(sec)	(sec)	(cm)	(cm/sec)	(mm/sec)	(Kpa)	(Kpa)	(Kpa)	(Kpa)	(Kpa)	(Kpa)
1	5	3,30	6	14	57	77	35	1	0,04						
2	5,2	3,10	2	7	9	18	37	5	0,18	366	504	518	538	524	469
3	6	3,20	1	8	40	49	28	1	0,07						
4	6	3,15	2	7	24	33	29	2	0,11						
5	6	3,18	2	7	18	27	29	3	0,15	455	559	580	600	593	573
6	7	3,20	5	9	49	63	24	1	0,08						
7	7	3,20	2	8	20	30	24	3	0,18	386	497	490	518	490	435
8	7,5	3,15	3	6	38	47	25	2	0,11						
9	8	3,25	2	6	46	54	21	2	0,10						
10	8	3,18	2	8	30	40	21	3	0,16	566	766	807	849	828	745
11	9	3,18	2	5	35	42	21	3	0,16						
12	9	3,20	2	5	31	38	18	2	0,19	580	780	794	828	828	725

Table 3.3 Data of each experiment with the OCF 8610

	Thickness		Cycle Time		Flow Front		In mold pressure at the end of injection					
Exp.	Initial	Final	Inj. Time	Clamp. Time	Average Flow Front speed	Closing Speed	P1 @ 1.8cm	P2 @ 14.8cm	P3 @ 25.5cm	P4 @ 36.3cm	P5 @ 47.0cm	P6 @ 57.8cm
(#)	(mm)	(mm)	(sec)	(sec)	(cm/sec)	(mm/sec)	(Kpa)	(Kpa)	(Kpa)	(Kpa)	(Kpa)	(Kpa)
1	5,0	3,3	19	25	2,9	0,08	166	n/a	145	n/a	n/a	95
2	5,1	3,1	18	25	3,2	0,08	153	123	99	74	47	19
3	5,0	3,2	17	25	3,6	0,08	162	159	138	131	124	124
4	5,0	3,2	21	24	2,7	0,09	170	182	166	153	130	130
5	5,2	3,2	16	24	3,7	0,09	166	143	119	98	69	66
6	5,1	3,2	20	24	2,9	0,09	178	187	170	160	128	96
7	5,1	3,2	21	21	2,8	0,09	172	179	164	155	135	121
AV.	**5,1**	**3,2**	**19**	**24**	**3,1**	**0,09**	**167**	**162**	**143**	**129**	**106**	**93**

CONCLUSION

La première partie de ce travail a porté sur l'étude des procédés de moulage RTM et SRIM dans la fabrication de pièces composites à coeur de mousse. Le système d'injection SRIM a permis de mesurer expérimentalement la déformation des coeurs de mousse de diverses densités, leurs déplacements ainsi que la compaction des renforts.

Les expérimentations SRIM avec le moule plaque ont permis de constater que pour une faible densité de mousse polyuréthanne, la déformation du noyau de mousse était non négligeable. La compaction des coeurs de mousse et de celle des renforts durant le moulage a pu être comparée avec les tests de compression indépendamment effectués sur une presse. Il semble que la distribution de pression évolue selon une régression linéaire pour les noyaux de mousse de faible densité. Les simulations effectuées à l'aide du logiciel RTMFLOT selon une loi de Darcy linéaire ont permis de donné une bonne approximation de la distribution de pression au point d'injection.

Les expérimentations SRIM utilisant le moule quasi rectangulaire ont démontré que le déplacement des coeurs de mousse ainsi que la compaction des renforts étaient les principaux problèmes, contrairement à la compression des noyaux de mousse. Des lamelles de bois utilisés sur la surface des coeurs de mousse ont effectivement réussi à réduire considérablement le déplacement

des noyaux ainsi que d'éliminer les zones sèches dues à la compaction des renforts. La tentative de prédire la compaction des renforts pour une pression donnée n'a procuré que des résultats approximatifs à l'aide de la mesure de compressibilité des renforts sur une presse indépendante. Les résultats ont également prouvé que la pièce la moins coûteuse et la plus légère n'est pas nécessairement celle possédant un coeur de mousse de faible densité.

La seconde partie de cet ouvrage a porté sur l'étude du procédé de moulage CRTM et de ses variantes possibles. Le moulage CRTM permet de fabriquer des pièces composites avec de hauts taux de fibres tout en utilisant un système d'injection à basse pression.

Les expérimentations utilisant une préforme thermoformée à l'épaisseur finale de la pièce dans un moule ouvert ont démontré la facilité et la rapidité avec laquelle il est possible d'injecter la résine. La fermeture du moule permet de bien mouiller le renfort et d'obtenir une pièce avec un taux de fibre élevé. Par contre, la fermeture de la presse peut engendrer une montée de pression importante dans le moule, particulièrement pour des préformes de verre d'épaisseur variable.

Le moulage CRTM utilisant des mats aléatoires continus avec un taux de fibre faible ne semble pas avoir un avantage marqué sur le procédé

conventionnel RTM. Par contre, le fait d'injecter la résine en même temps que le moule est fermé permet d'étudier une loi de Darcy non-linéaire durant le remplissage du moule. Également, cette approche permettra de mieux comprendre le moulage de pièces composites en coeur de mousse.

BIBLIOGRAPHIE

1. **JÖNSSON, K. A.-S., JÖNSSON, T.L.** (1992). « Fluid flow in compression porous media I : Steady-state conditions », *AIChE Journal, 38, 9,* 1340-1348.
2. **JÖNSSON, K. A.-S., JÖNSSON, T.L.** (1992). « Fluid flow in compression porous media II : Dynamic Behavior », *AIChE Journal, 38, 9,* 1349-1356.
3. **DARCY, H.** (1856). « Les fontaines publiques de la ville de Dijon », *Dalmont, Paris.*
4. **LEBRUN, G.** (1995). « Étude des phénomènes d'échanges thermiques dans le procédé de moulage par transfert de résine (RTM). », *Thèse Ph.D, École Polytechnique de Montréal,* 31-34.
5. **GREENKORN, R.A.** (1983). « Flow phenomena in porous media », *Marcel Dekker, New-York.*
6. **WISSLER, E. H.** (1971). « Viscoelastic effects of the flow of non-newtonian fluids through a porous medium », *Ind. Eng. Chem. Fundam., 10,* 411-417.
7. **PARNAS, R.S., PHELAN, Jr. R. R.** (1991). « The effect of heterogeneous porous media on mold filling in resin transfer molding », *SAMPE Quartely, Jan.,* 53-60.

8. **GUTOWSKI, T. G., MORIGAKI, T., CAI, Z.** (1987). « The consolidation of laminate composites », *Journal of Composite Materials, 21,* 172-188.

9. **GUTOWSKI, T. G., CAI, Z., BAUER, S., BOUCHER, D., KINGERY, J., WINEMAN, S.** (1987). « Consolidation experiments for laminate composites », *Journal of Composite Materials, 21,* 650-669.

10. **HAN, K., TREVINO, L., LEE, L. J., LIOU, M.** (1993). « Fiber mat defromation in liquid composite molding I : Experimental analysis », *Polymer Composites, 14, 2,* 144-150.

11. **HAN, K., LEE, L. J., LIOU, M.** (1993). « Fiber mat defromation in liquid composite molding II : Modeling », *Polymer Composites, 14, 2,* 150-160.

12. **GUTOWSKI, T. G.** (1985). « A resin flow/fiber deformation model for composites », *SAMPE Quaterly, jul.,* 58-64.

13. **BAKALÉMIAN, P.-Y.** (1995). « Caractérisation de l'effet de bord et de la compressibilité des renforts pour le procédé de moulage par transfert de résine (RTM) », *CRASP, École Polytechnique de Montréal.*

14. **GAUVIN, R., TROCHU, F.** (1994). « RTMFLOT, un logiciel intégré de modélisation des procédés RTM et SRIM », *COMPOSITES, 5,* 16-22.

15. **FONG, L., LEE, L. J.** (1994). « Preforming analysis of thermoformable fiber mats - Preforming effects on mold filling », *Journal of Rein. Plas. And Comp., 13,* 637-663.

16. **GAUVIN, R., CHIBANI, M.** (1988). « Modelization of clamping force and mold filling in resin transfer molding », *43rd Annual Conf., Comp. Inst., Soc. Plas. Ind., Feb. 1-5.*

17. **GAUVIN, R., CHIBANI, M., LAFONTAINE, P.** (1986). « The modeling of pressure distribution in resin transfer molding », *41rd Annual Conf., Comp. Inst., Soc. Plas. Ind., Jan. 27-31.*

18. **MARTIN G. Q., SON, J. S.** (1986). « Fluid mechanics of mold filling for reinforced plastics », *Proceedings, ASM/ESD Sec. Conf. Adv. Comp., 149.*

19. **TREVINO, L., LEE, L. J., RUPEL, K., LIOU, M. J.** (1990). « Permeability and compressibility measurement of fiber mats in resin transfer molding ands structural RIM », *45rd Annual Conf., Comp. Inst., Soc. Plas. Ind., Feb. 12-15.*

20. **BATCH, G. L., CUMISKEY, S.** (1990). « Multilayer compaction and flow in composites processing », *45rd Annual Conf., Comp. Inst., Soc. Plas. Ind., Feb. 12-15.*

21. **GEBART, B. R.** (1992). « Permeability of unidirectional reinforcements for RTM », *Journal of Composites Materials, 26, 8,* 1100-1133.

22. **FERLAND, P., GUITTARD, D., TROCHU, F.** (1995). « Concurrent methods for permeability measurement in resin transfer molding », *Polymer Composites, March.*

23. **GAUVIN, R., CLERK, P., LEMENN, Y., TROCHU, F.** (1994). « Compaction and creep behavior of glass reinforcement for liquid

composites molding », *10th Annual ASM/ESD Adv. Comp. Conf., Dearborn, MI,* 357-367.

24 **KENDALL, K.N. RUDD, C.D. OWEN, M.J. MIDDLETON, V.** (1992). « Characterization of the resin transfer moulding process », *Composites Manufacturing, **3**, 4,* 235-247.

25 **KENDALL, K.N.** (1994). « Component and Process Design for Liquid Composite Moulding », *Int. Conf. on design and manufacturing using Composites, ATNAM '94, Montreal.*

26 **C.F. JOHNSON, N.G. CHAVKA, R.A., JEYRON.** (1986). « Resin Transfer Moulding of Complex Automobile Structures », *Proceeding of 41st Annual Conf. of the Reinf. Plastics Comp. Inst., Society of the Plastics Industry Inc., session 12-A.*

27 **C.D. RUDD, E.V. RICE, L.J. BULMER, A.C. LONG.** (1993). « Process Modelling and Design for Resin Transfer Molding », *Plactic, Rubber and Composites Processing and Applications, **20**, 2,* 67-76.

28 **GAUVIN, R. and CHIBANI**, (1986). « The Modeling of Mold Filling in Resin Transfer Molding », *International Polymer Processing, **1**, 1,* 42-46.

29 **GAUVIN, R., TROCHU, F.** (1996). « Keys Issues in Numerical Simulation of Liquid Composites Molding Processes », *Proc. Of the 29th ISATA Conf.,* 1107-1114.

30 **W.B YOUND, K. HAN, L.H. FONG, L.J. LEE, M.J. LIOU.** (1991). « Flow Simulation in Molds with pre-placed Fiber Mats », *Polymer Composites, **12**, 6,* 391-403.

31 **D.A. BABBINGTON, J.H. ENOS, J.M. COX.** (1987). « High Speed RTM of Vinyl Ester Resins », *AUTOCOM-87, Dearborn, MI, EM87-351.*

ANNEXE I

MOULAGE CRTM D'UNE PRÉFORME DE TISSU J .B. MARTIN

Les résultats suivants sont la suite des expérimentations du chapitre 3 utilisant une préforme de tissu J.B. Martin 82001-A au lieu d'une préforme Brochier. Le tissu J.B. Martin a été thermoformée à l'épaisseur finale constante de la pièce (3.1mm). La préforme est ensuite déposée dans un moule plaque rectangulaire légèrement ouvert, laissant un canal vide entre la paroi supérieure du moule et la surface de la préforme. La résine est injectée dans la cavité vide et par la suite le moule est fermé, permettant un mouillage uniforme de la préforme.

La figure I.1 représente la courbe typique de compressibilité de 10 couches de tissu J.B. Martin. La figure I.2 représente le mouillage du tissu durant l'injection de la résine et la fermeture du moule. Les résultats ne sont pas concluants en ce qui concerne l'influence de la hauteur de cavité sur le remplissage du moule. La figure I.3 démontre l'influence de la hauteur de la cavité en fonction de l'avancement du front d'écoulement de la résine. Enfin, la figure I.4 donne la variation de la hauteur de la cavité en fonction du temps permettant de calculer la vitesse de descente du plateau de la presse. Le tableau I.1 résume les donnés obtenus lors des expérimentations effectuées avec la préforme de tissu J.B. Martin.

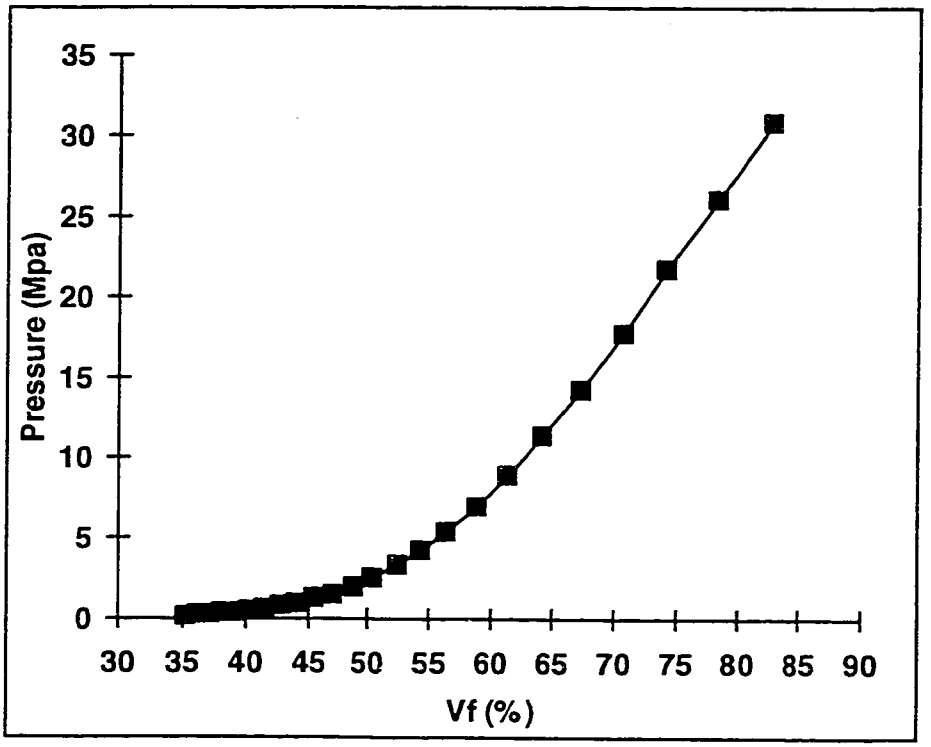

Figure I.1 Compressibility test of 10 layers of J.B. Martin 82001-A

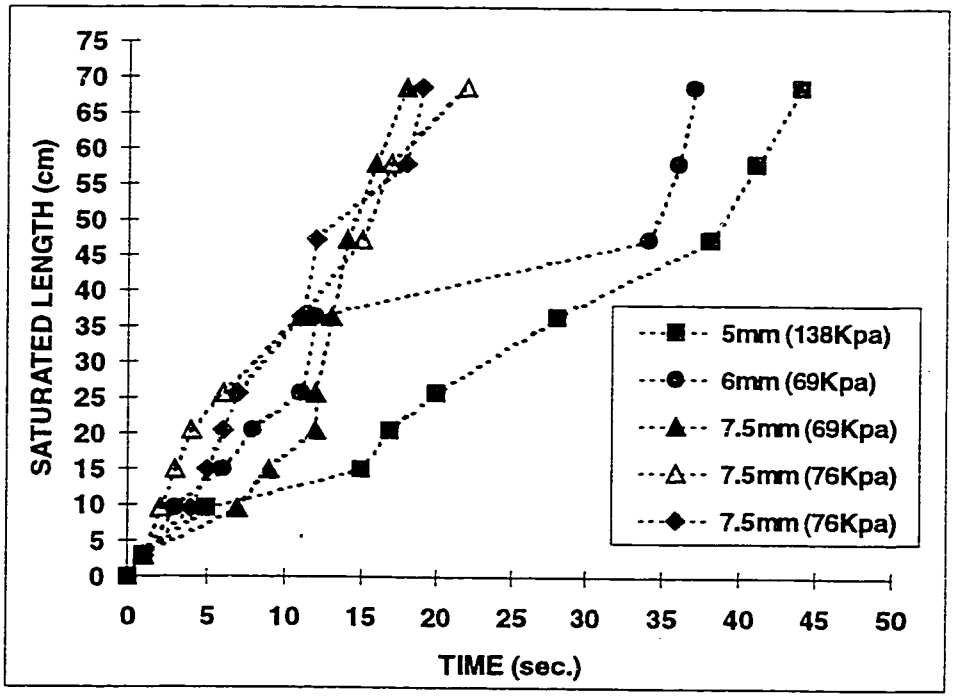

Figure I.2 Saturated length versus time for the J.B. Martin 82001-A preform with a V_f of 30%

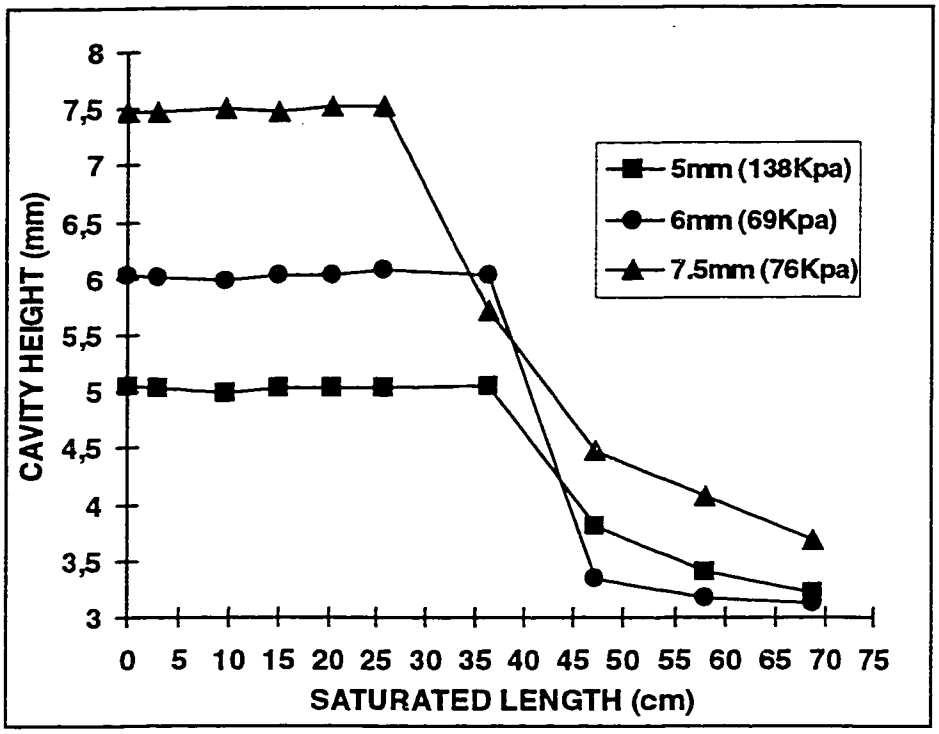

Figure I.3 Cavity height versus saturated length for experiments with the J.B. Martin preform

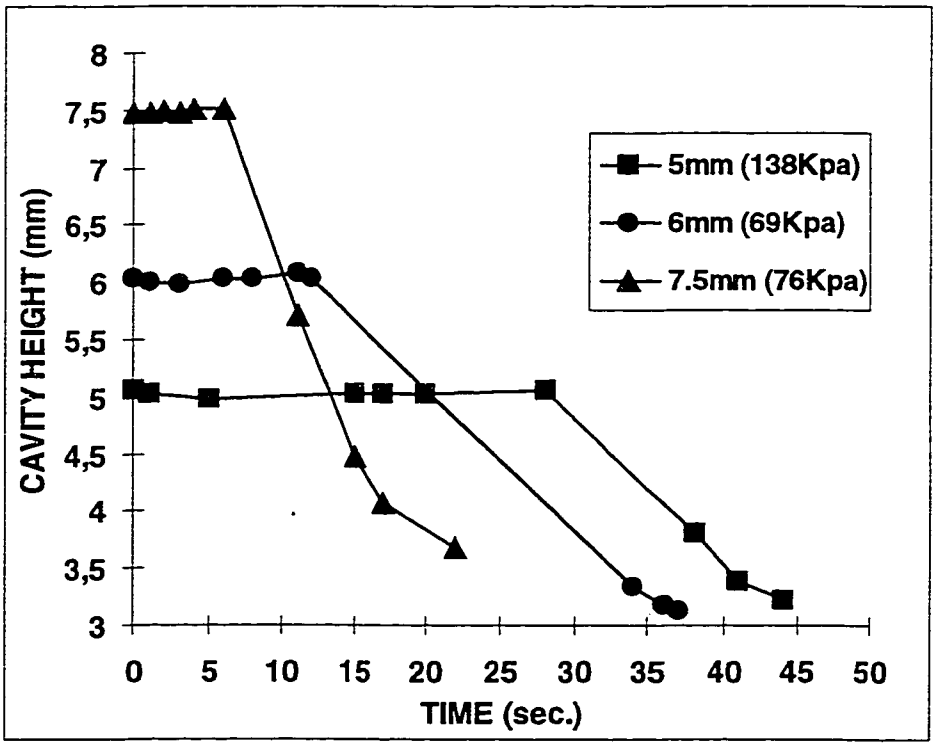

Figure I.4 Cavity height versus time for J.B. Martin preform

Table I.1 Data of each experiment with J.B. Martin 82001-A preform

		Thickness		Cycle Time				Resin Flow Front		
Exp.	Inj. Press.	Initial	Final	Inj. Time	Wait Time	Clamp. Time	Cycle Time	Location in the Gap Before Clamping	Average speed	Closing speed
(#)	(Kpa)	(mm)	(mm)	(sec)	(sec)	(sec)	(sec)	(cm)	(cm/sec)	(mm/sec)
1	138	5	3.2	29	6	13	48	35	0.2	1.6
2	69	6	3.1	10	22	5	37	25	0.7	1.9
3	69	7.5	3.1	3	7	8	18	22	0.7	3.8
4	76	7.5	3.5	3	5	27	35	22	0.3	3.1
5	76	7.5	3.7	2	10	28	40	22	0.2	3.6

IMAGE EVALUATION
TEST TARGET (QA-3)

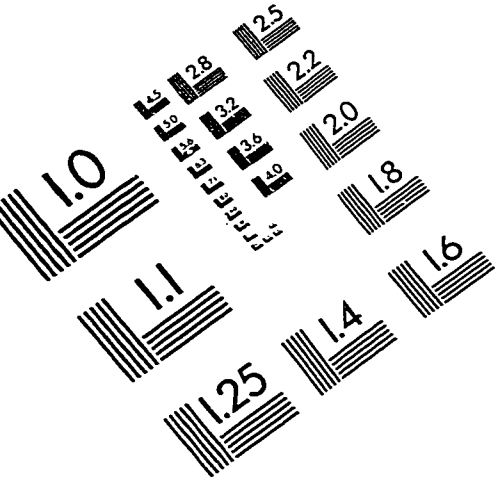

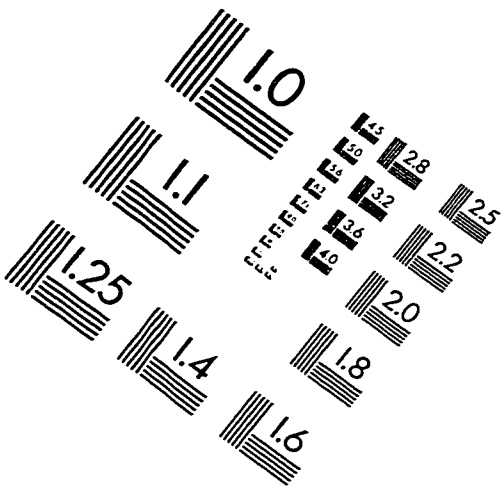

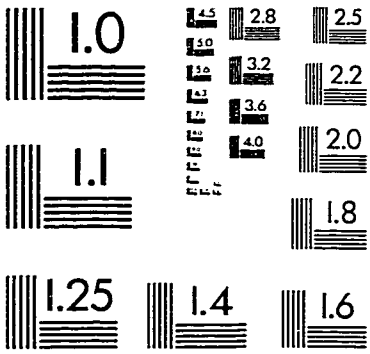

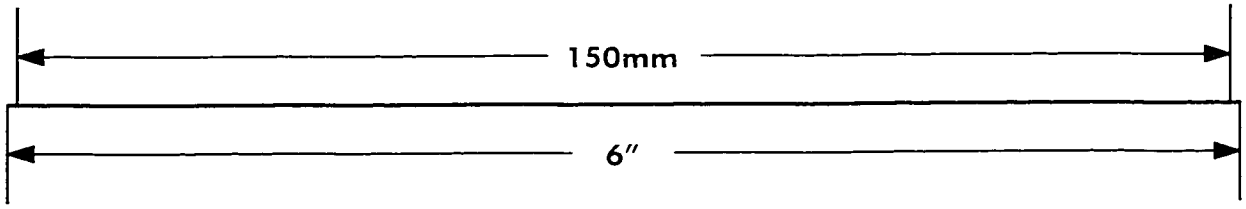

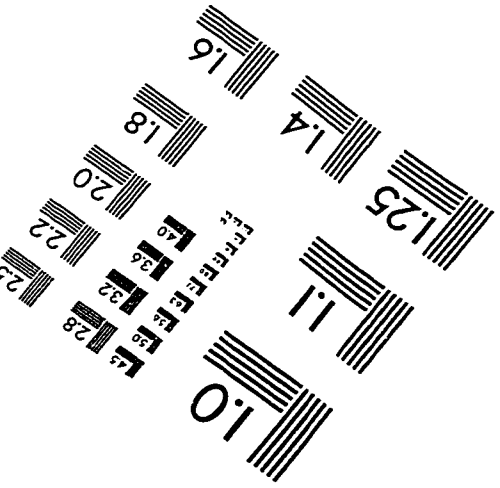

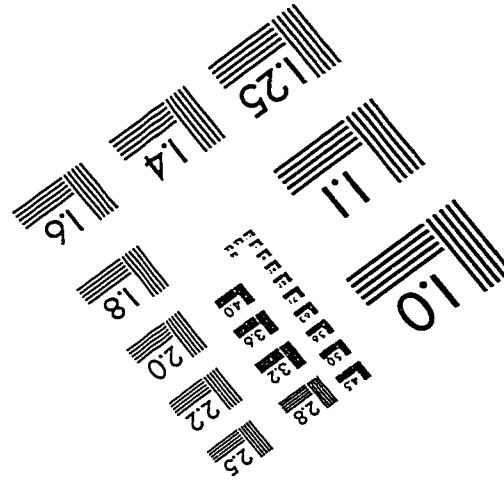

APPLIED IMAGE, Inc
1653 East Main Street
Rochester, NY 14609 USA
Phone: 716/482-0300
Fax: 716/288-5989